UNIVERSITÀ
DEGLI STUDI
DI TORINO

AALBORG UNIVERSITY
DENMARK

Università degli Studi di Torino in collaboration with

Aalborg University

Master's Degree in "Industrial Chemistry"

MASTER THESIS

COMPARISON OF CHEMICAL CROSS-LINKERS WITH BRANCHED AND LINEAR MOLECULAR STRUCTURES FOR STABILIZATION OF GRAPHENE OXIDE MEMBRANES AND THEIR PERFORMANCE IN ETHANOL DEHYDRATION

Candidate
Luca Calzavarini

Supervisor
Prof.ssaMagnacca Giuliana

Co-supervisor
Prof. Boffa Vittorio

Examiner
Prof. Laurenti Enzo

Academic Year 2018/2019

SUMMARY

Abstract **4**

Introduction **5**

1. STATE of ART **8**

1.1 Membrane Separation Process 9
1.1.1 Membranes Classifications 10
1.1.2 Governing Parameters for Membranes Performance 13
1.1.3 Membrane Shapes and Flow Geometries 15
1.1.4 Disadvantages – Polarization and Fouling 17
1.2 Membrane Technology in Energy Sustainability 19
1.2.1 Biofuels 20
1.2.2 Membrane Technology in Biofuels Production and Purification 22
1.3 Graphene-Oxide Membranes 29
1.3.1 GO Structure 30
1.3.2 GO Synthesis 32
1.3.3 GO Characterization 34
1.3.4 GO-based Membranes 37
1.3.5 GO Stabilization 42

2. EXPERIMENTAL SECTION **46**

2.1 Materials 46
2.2 Graphene-Oxide (GO) 47
2.2.1 Synthesis 47
2.2.2 Characterization 48
2.3 Preparation of free-standing cross-linked GO films 51
2.4 Stability Studies 53
2.5 Preparation of large-area supported GO films 55
2.6 Vapour permeation Studies 56

2.6.1 Determination of permeance of water and ethanol 56
2.6.2 Dehydration of ethanol-water misture 56

3. RESULTS and DISCUSSION 59

3.1 Graphene-Oxide Characterization 59
3.2 Stabilization of GO with Different Cross-Linkers 60
3.2.1 Polyethylene Glycol 61
3.2.2 Synthetic Hyperbranched Polyol (HBPO) 73
3.2.3 Humic Acid-Like Substances (HAL) 77
3.3 Vapour Permeation Experiments 80
3.3.1 Permeation of Water and Ethanol 82
3.3.2 Dehydration of Water/Ethanol Mixture 87

4. CONCLUSIONS 91

References 93

Acknowledgments 98

ABSTRACT

In this thesis it will be reported the fabrication of large-area cross-linked Graphene-Oxide (GO) membranes by rod coating and their use for dehydration of ethanol by vapor permeation.

The first part of the project was focused on the synthesis of GO and its characterization by X-Ray Diffraction and Raman Spectroscopy.

Once confirmed the successful synthesis of GO, two cross-linker species with branched structures, humic acid-like substances derived from urban waste (HAL) and a synthetic hyperbranched polyol (HBPO), have been used with the aim of stabilizing GO. For comparison, a previously reported cross-linker, poly(ethylene glycol) (PEG), has also been used. At first, free-standing cross-linked membranes with various ratios of cross-linker-GO were subjected to submergence in water and tumbling for 24 hours, in order to determine the composition required to produce stable membranes. The effect of the incorporation of cross-linker on the spacing between GO layers was studied by X-ray diffraction analysis of free-standing membranes both before and after the submergence test; UV-vis spectroscopy on the water containing the free-standing films was performed in order to determine the concentration of GO dissolved in water.

In the last part of the project supported cross-linked GO films were prepared by rod coating on polyethersulphone ultrafiltration membrane. Preliminary studies of their performance in water and ethanol vapor permeation as well as for dehydration of ethanol/water mixture were carried out.

INTRODUCTION

The development of our society is closely linked to energy consumption; without Energy men would never have managed to reach the level of well-being and quality of life they now have and, without the availability of sufficient Energy resources, future economic development would be compromised.

The *Energy Issue* has always occupied a leading position in the global economy and development. Fossil fuels such as oil, coal and natural gases have become the prime sources of energy in the current era. As shown in Figure 1, more than the 80% of the Energy currently used comes from fossil fuels. However, these resources have been long presupposed as abundant. With the increase of population and the developments brought by the industrial revolution, their demand increased and scarcity is now an undeniable result. The current global energy problem originates not only from limited fossil energy supplies, but also its environmental impacts for its entire energy lifecycle, from mining and processing to emissions, waste disposal and recycling. The indicators of energy sustainability include its price, environmental impacts and greenhouse gas emissions, availability of renewable energy sources, land requirements, water consumption and social impacts. One solution to achieve energy sustainability is to develop sustainable technologies to gradually replace non-renewable fossil fuels. These include energy conversion from renewable and/or natural resources, such as biomass, wind, solar and water, into usable energy and energy storage systems for long-term or remote usage. Bioethanol, or ethanol produced from biomass, is being regarded as a viable alternative to fossil fuels. However, fermentation of biomass produces ethanol with high water content, and the

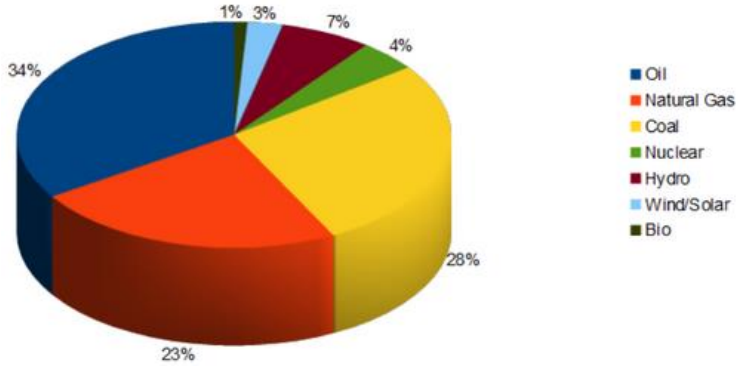

FIGURE 2 GLOBAL ENERGY CONSUMPTION IN 2017

azeotrope formed by ethanol with water at 1 atm and 78.2°C at 89.4 mole *per cent* (corresponding to 95.6 $\%_w$) of ethanol presents a hurdle in the way of the production of anhydrous ethanol required for use as fuel. Numerous techniques are being explored for the dehydration of bioethanol, including azeotropic distillation, vacuum distillation and chemical desiccation.

Among all the possible technologies, membrane technology plays a key role in this area. As a matter of fact, besides addressing Energy scarcity, membrane technologies meet sustainability criteria in terms of environmental impacts, land usage, ease of use, flexibility and adaptability. However, they still need to be improved in terms of cost and affordability, energy consumption and expertise. To achieve these improvements, advances in membrane materials are needed.

Recently, carbon-based materials have shown considerable potential in field of membrane separation. Graphene-Oxide (GO), derived from natural graphite, in particular, has been used as one of the emerging materials for the production of new membranes. As a matter of fact, as shown in Figure 2, in recent decades, patents and papers, including review papers and research articles, focusing on GO-based membranes are grown exponentially.

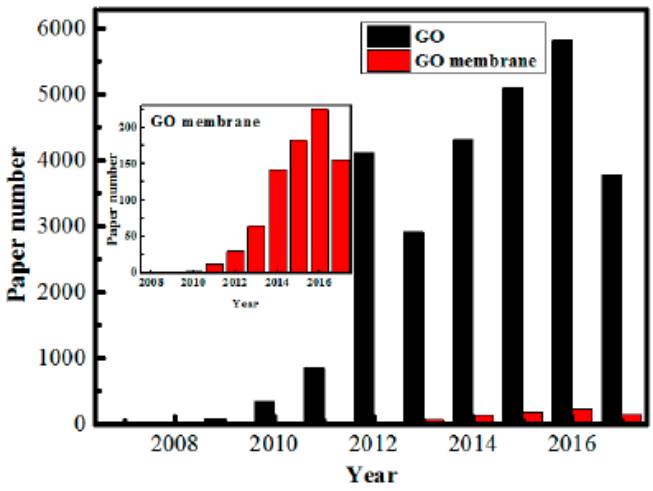

FIGURE 2 NUMBERS OF PUBLICATION FOR GO AND GO-BASED MEMBRANES (2008-2017)

Unimpeded water permeation and high selectivity towards organic molecules have recently been reported for GO-based thin films [1], thus unlocking a new and exciting direction in the development of artificial membranes for different applications, including alcohol dehydration technologies.

At present, despite significant advancements in GO-based membranes have been achieved, a few critical challenges in realizing real-world application of GO-based membranes still exist. Specifically, the instability of the inter-layer spacing between adjacent GO nanosheets is a great challenge for utilizing laminar GO membranes as selective aqueous separation barriers, especially for water-related treatment. This is because GO membrane easily disintegrated and redispersed in water over time due to the highly hydrophilic nature of the GO sheets and electrostatic repulsion between the negatively charged GO sheets on hydration and then the integrity of the laminar GO membranes and inter-layer nanochannels formed by stacking GO sheets would be damaged. Therefore, it is very much desirable to enhance the structural stability of GO membrane by forming stable bonding between GO nanosheets to realize real-world applications of GO membranes in aqueous separation processes [2].

In this thesis project the possible stabilizing effects on GO, previously synthesized and characterized, of three different chemical cross-linkers with branched and linear molecular structure are analyzed. Later, the production of large-area cross-linked GO membranes are produced by rod coating, supporting GO on a polyethersulphone ultrafiltration membrane, and their performance in water and ethanol vapor permeation as well as for drying of ethanol are studied.

1. STATE OF ART

Water and energy are fundamental resources used for economic, social and cultural development. These resources have been long presupposed as abundant but, with the increase of population and the developments brought by the industrial revolution, their demand increased and scarcity is now an undeniable result.

In Figure 1.1 is possible to see the total global stock of water for human use [3]. From the global water reserve, only 2.5% is fresh water and the rest is saline. From the 2.5% the largest part is frozen in polar regions and 30% are also in remote aquifers of difficult access. As a result, only 0.007% of the total global water is directly accessible for use. Unfortunately, part of this water is polluted by industrial plants, mining, oil or gas exploration, fertilizer and pesticide residue used in agriculture. In addition, the uneven distribution of water over the globe causes even more severe water scarcity in some regions. Desalination and water reclamation are of paramount importance in water security, where desalination happens to be one of the main life supports in many arid regions.

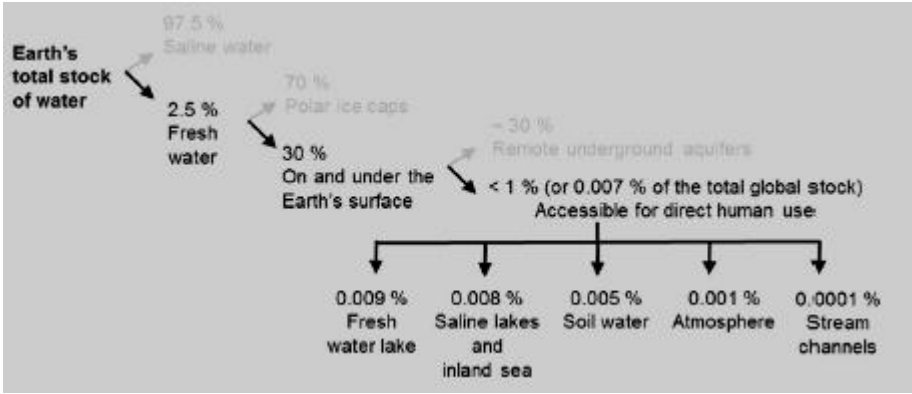

FIGURE 1.1 THE TOTAL GLOBAL STOCK OF FRESH WATER FOR HUMAN USE

The current global energy problem originates not only from limited fossil energy supplies, but also from its environmental impacts for its entire energy lifecycle, from

mining and processing to emissions, waste disposal and recycling. The indicators of energy sustainability include its price, environmental impacts and greenhouse gas emissions, availability of renewable energy sources, land requirements, water consumption and social impacts [4]. One solution to achieve energy sustainability is to develop sustainable technologies to gradually replace non-renewable fossil fuels. They include energy conversion from renewable and/or natural resources (e.g. biomass, wind, solar and water) into usable energy (e.g. electricity) and energy storage systems for long-term or remote usage.

Membrane technologies play a significant role in water and Energy sustainability. Some of them are already applied in industries at scale. Examples include desalination by reverse osmosis (RO), wastewater treatment by membrane reactors (MBR), lithium–ion batteries and membrane-based fuel cells. Besides addressing water and energy scarcity, membrane technologies meet sustainability criteria in terms of environmental impacts, land usage, ease of use, flexibility and adaptability. On the other hand, they still need to be improved in terms of cost and affordability, energy consumption and expertise. To achieve these improvements, advances in membrane materials are needed.

1.1 MEMBRANE SEPARATION PROCESS

Membrane separation processes have a very important role in the separation field. They cover a group of separation processes in which the characteristics of a membrane are used to separate the components of a solution or a suspension. In these processes the feed stream is separated into two parts: the fraction that permeates through the membrane, called *permeate*, and the fraction containing the components that have not been transported through the membrane, called *retentate.*

Two basic models can be distinguished for mass transfer through the membrane:

- The *Solution-Diffusion Model*: transport occurs only by diffusion and the component that needs to be transported must first be dissolved in the membrane. The general approach of the solution-diffusion model is to assume that the chemical potential of the feed and permeate fluids are in equilibrium with the adjacent membrane surfaces such that appropriate expressions for the chemical potential in the fluid and membrane phases can be equated at the solution-membrane interface.
- The *Hydrodynamic Model*: Transport through pores is done convectively. This requires the size of the pores to be smaller than the diameter of one of the two separated components.

1.1.1 MEMBRANES CLASSIFICATIONS

The main element in membrane separation process is the membrane itself. However, the term *membrane* is generally referred to different selective setups with very different characteristics. For this reason, we refer to various classifications carried out according to characteristic parameters of the membrane. More precisely, membranes are classified according to:

- The **material** they are made of. Membranes can be:
  - *Organic* or *Inorganic*;
  - *Natural* or *Synthetic*;
  - In *solid* or *liquid state*

- Based on their **structure**, membranes can be classified in:

  - *Symmetric*: the membrane is characterized by a symmetrical channel structure. They are not so much used cause of pores clogging problems;
  - *Asymmetric*: these kind of membranes are composed by a more dense layer with a thickness of 0,1-0,5 μm leaning on a thicker support layer (150-200 μm);
  - *Composite*: obtained by spreading a thin film on an asymmetric membrane having small pores

- The effective **porosity** of a membrane represents its capacity for detention. Through the use of porosimetric techniques, it is possible to establish in statistical terms an average pore size and then go back to the porosity through the knowledge of the pore density. Depending on the size of porosity, membranes are classified in:

  - *Porous membranes*: the pore size is between 1 nm and 10 μm. They can be further divided in macroporous (pore size > 50 nm), mesoporous (pore size between 2 and 50 nm) and microporous (pore size < 2 nm);
  - *Dense membranes*: characterized by a pore size < 1 nm

  The mechanism of separation of these two kinds of membranes is different, as a matter of fact porous membranes act like a sieve that allows the passage of the only particles of smaller size than that of the pores. Dense membranes separate substances according to their different solubility and diffusion through the dense layer.

- The **molecular weight of the retentate**, also known as MWCO (*Molecular Weight Cut-Off*) is linked to the dimension of the retained material depending on the characteristics of the membrane. It is defined as the minimum molecular weight of a globular molecule that is retained to 90% by the membrane. The cut-off, depending on the method, can be converted to the so-

called D_{90}, which is then expressed in a metric unit. In practice, the MWCO of the membrane should be at least 20% lower than the molecular weight of the molecule that is to be separated.

- Depending on the **driving force** that allows transport of material through the membrane, membrane processes can be divided in several big categories:

  - *Filtration*, based on a pressure gradient. Filtration process uses variable pressure differences to allow the passage of the permeate beyond the membrane through the pores that compose it. Depending on the pore size, filtration processes are so called:

    - ✓ *Microfiltration (MF)*: used for the removal of suspended particles, pigments, emulsions and bacteria;
    - ✓ *Ultrafiltration (UF)*: used for the removal of bacteria, virus and proteins;
    - ✓ *Nanofiltration (NF)*: used for the removal of molecules;
    - ✓ *Iperfiltration (IF)* or *Reverse Osmosis (RO)*: used for the removal of ions, desalination of drinking water and water purification for industrial and pharmaceutical purposes

    From MF to IF, there is a decrease in the pore size and an increase in the pressure gradient applied.

  - *Electrodialysis*, based on application of an electric field. It allows the separation of an ionic solute from a solution through the use of electric Energy and cationic or anionic permeable membranes, depending on the charge of the ion that needs to be separated.

  - *Pervaporation and Vapor Permeation* [5]: for both of this kind of separation the driving force is a gradient in chemical potential which is established by applying a difference in partial pressure of the

permeants across the membrane. Pervaporation is recognized as a separation process in which a binary or multicomponent liquid mixture is separated by partial vaporization through a dense non-porous membrane. During pervaporation, the feed mixture is in direct contact with one side of the membrane whereas the permeate is removed in a vapor state from the opposite side into a vacuum or sweeping gas and then condenses. Vapor permeation is similar in principle to pervaporation. The only difference concerns the feed, which is a mixture of vapors or vapors and gases. Thus, compared to pervaporation, the addition of heat equivalent to the enthalpy of vaporization is not required in the membrane unit and there is no temperature drop along the membrane. Operation in the vapor phase also eliminates the effect of the concentration polarization prevalent in liquid phase separations, such as pervaporation.

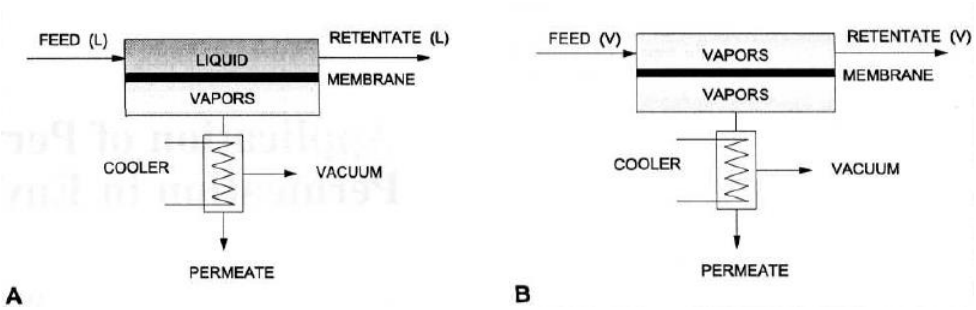

FIGURE 1.2 SCHEMA OF (A) PERVAPORATION AND (B) VAPOR PERMEATION PROCESS

1.1.2 GOVERNING PARAMETERS FOR MEMBRANES PERFORMANCE

The selection of membranes for a targeted separation process is usually based on few requirements:

- Membranes have to provide enough mass transfer area to process large amounts of feed stream;

- The selected membrane has to have high selectivity properties for certain particles;
- It has to resist fouling and to have high mechanical stability;
- It also needs to be reproducible in its behaviors and to have low manufacturing costs.

The efficiency of a membrane is usually described in terms of *permeance* and *selectivity.*

Permeance is considered as the ratio between the flux of a determined species through the membrane and the difference in its partial pressure between the two faces of the membrane. This parameter allows the comparison between the results obtained analyzing the same membrane using different partial pressures.

$$P_i = {J_i}/{\Delta p_i}$$

The membrane ***selectivity*** is a parameter used to compare the separating capacity of a membrane for two or more species. The selectivity, also known as permselectivity or separation factor, of one component over another component is given by the ratio of their permeabilities:

$$\alpha_{ij} = {F_i}/{F_j}$$

Permeability of a species through the membrane is considered as the product of its permeance for the thickness of the membrane (L):

$$F_i = P_i * L$$

Permeance and selectivity are characterized by opposite trends: an increase in one of the two parameters causes a decrease of the other one, as shown in Figure 1.3.

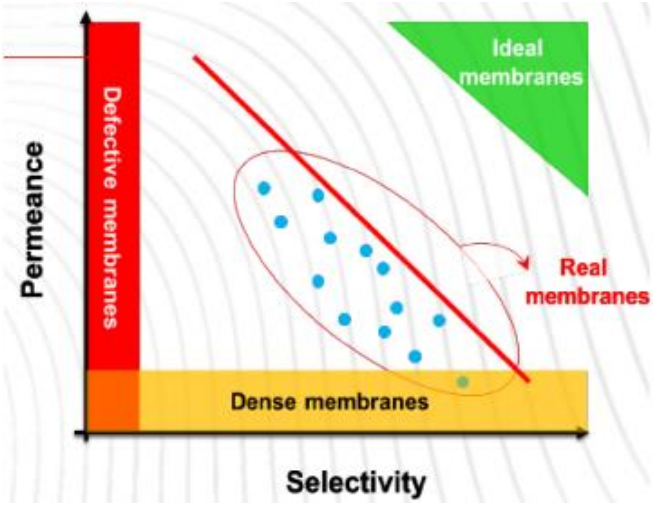

FIGURA 1.3 SELECTIVITY-PERMEANCE TREND

1.1.3 MEMBRANE SHAPES AND FLOW GEOMETRIES

Membranes are usually set on suitable supports to which the feed and drain pipes are connected. With the term *module* we refer to the smallest unit containing one or more membranes with their support structures that can operate independently from the rest of the system. The geometry of the module is such as to increase the specific surface of the membrane and minimize defects like fouling (this phenomenon will be explained in the next paragraph).

The main types of modules are:

- *Spiral Wound*: modules consisting of a series of pairs of flat membranes glued together and wrapped around a central channel for the permeate collection;

- *Hollow Fine Fiber*: these are modules made up of small tubes of materials with an asymmetrical structure having a thickness less than 0,1 μm inserted inside a pressure tube;
- *Plate and Frame*: each membrane is placed on a flat support with a drainage grid interposed to avoid the crushing of the permeate compartment. Various units of this type are assembled together and included in modules with channels for the feed and permeate collection;
- *Tubular*: the membrane is placed on the inner wall of a porous tube composed by a plastic material. More elements of this type are assembled together in order to produce a module. The feed flows inside each porous tube, the permeate leaves from the side and it is collected by the outer casing.

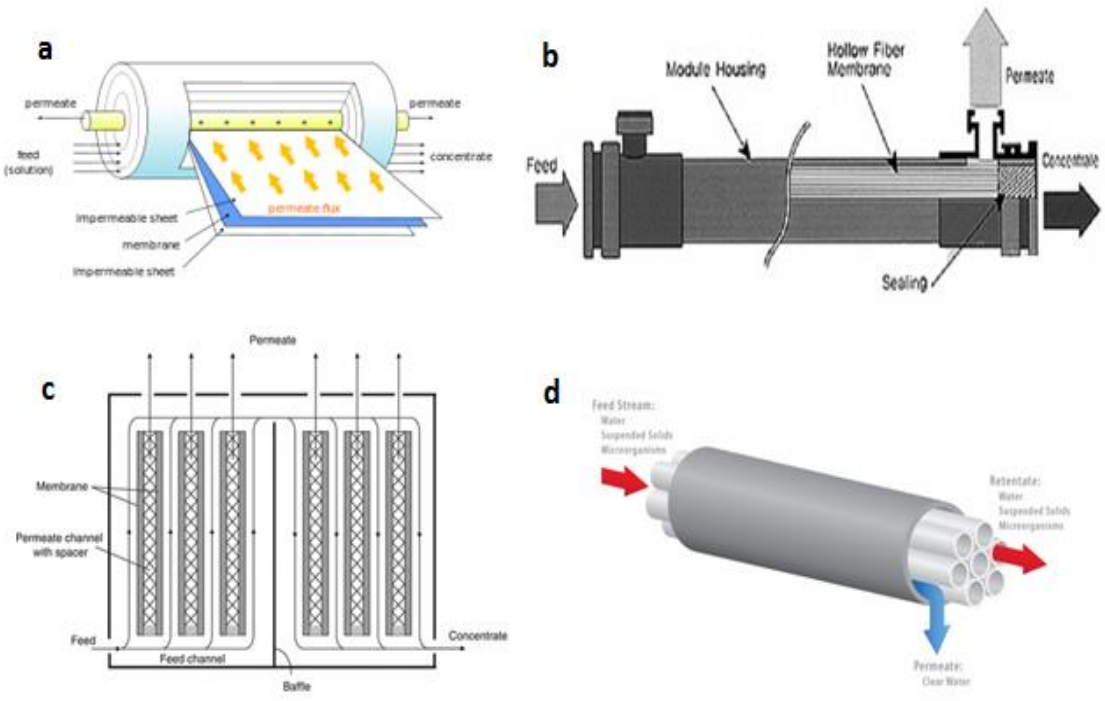

FIGURE 1.4 (a) SPIRAL WOUND (b) HOLLOW FINE FIBER (c) PLATE AND FRAME (d) TUBULAR MODULES

The modules described above can be connected according to the process requirements. There are two main flow configurations of membrane processes, as shown in Figure 1.5:

– *Cross Flow Filtration*: the feed flow is tangential to the surface of membrane, retentate is removed from the same side further downstream, whereas the permeate flow is tracked on the other side. This kind of devices are more expensive and labor-intensive, but they are less susceptible to fouling due to the sweeping effects and high shear rates of the passing flow.

– *Dead-end Filtration*: the direction of the fluid flow is normal to the membrane surface. This kind of membranes are relatively easy to fabricate which reduces the cost of the separation process. The separation process is easy to implement and the process is usually cheaper than cross-flow membrane filtration. The dead-end filtration process is usually a batch-type process, where the filtering solution is loaded (or slowly fed) into the membrane device, which then allows passage of some particles subjected to the driving force. The main disadvantage of this geometry is the extensive membrane fouling.

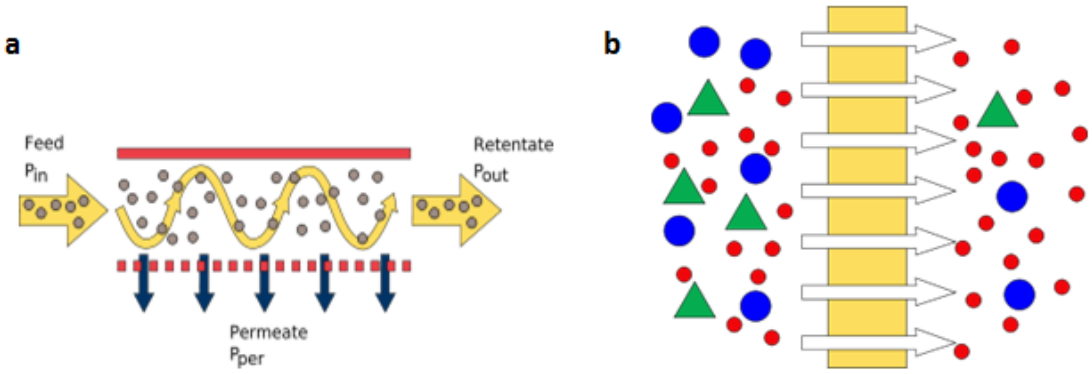

FIGURE 1.5 (A) CROSS-FLOW FILTRATION (B) DEAD-END FILTRATION

1.1.4 DISADVANTAGES – POLARIZATION AND FOULING

During membrane process, even if all the operative conditions are kept constant, a decrease in permeate flux can occur over time. The causes of these decrease can be identified in two phenomena: *concentration polarization* and *fouling*.

The first is characterized by an increase in solute concentration in the laminar boundary layer in contact with the membrane. Because of this, a higher local osmotic pressure is produced and a decrease in the driving pressure variation is identified. This leads to a decrease in the flux according to the osmotic pressure model:

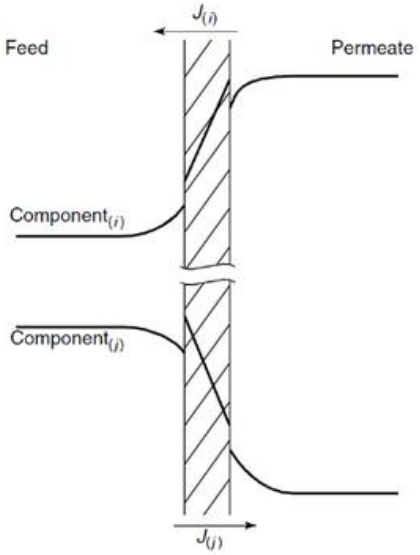

$$J = {(\Delta p - \Delta \pi)}/{R_m}$$

FIGURE 1.6 CONCENTRATION POLARIZATION ACCORDING TO THE OSMOTIC PRESSURE MODEL

Where:

- J is the flux piezometric decrease;
- Δp represents the driving force;
- Δπ is the osmotic pressure;
- R_m is the membrane resistance measured with reference to pure water

The importance of concentration polarization depends on the membrane separation process. It can significantly affect membranes performance in reverse osmosis but is usually well controlled in industrial systems. On the other hand, membrane performance in UF, electrodialysis and some pervaporation processes is seriously affected by concentration polarization. Anyway, this phenomenon is reversible just changing the operative conditions.

On the other hand, fouling is not reversible and, above all, it is much more problematic compared to the polarization. It derives from the deposition and accumulation of particles on the surface of the membrane and from the crystallization and precipitation of solute between the pores of the membrane itself. As a consequence, a layer acting as a secondary membrane is produced on the surface of the membrane reducing the flux. There are different methods used for delaying or minimizing this phenomenon such as:

- Treat the feed in order to remove that elements that may lead to a higher fouling degree like suspended particles;
- Keeping the feed under stirring;
- Working while keeping the membrane in vibration;
- Inverting the flux pattern in order to allow the detachment of the layer from the surface of the membrane

Anyway, as it is possible to see looking at the plot shown in Figure 1.7 there is never a total recovery of membrane functionality.

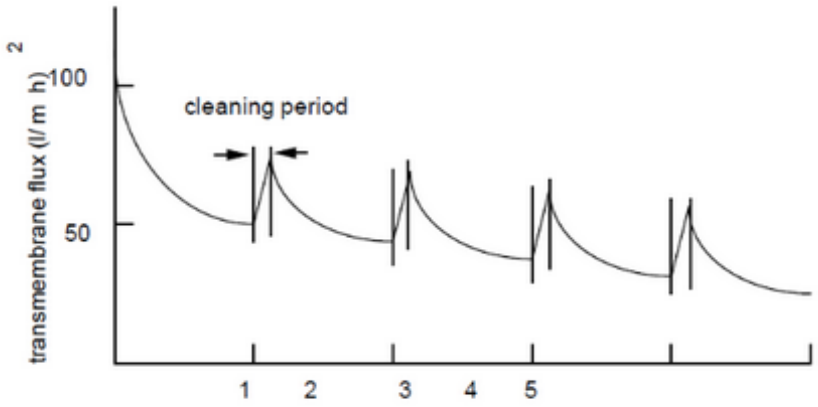

FIGURE 1.7 EFFECT OF FOULING ON TRANSMEMBRANE FLUX OVER TIME

1.2 MEMBRANE TECHNOLOGY IN ENERGY SUSTAINABILITY

Renewable energy sources are increasingly becoming a greater part of the global energy picture, particularly for power generation. They contributed approximately 58.5% of additions to the world's power generation capacity in 2014 with significant growth in all regions [6]. Membrane technology has a great potential to take advantages of renewable to produce energy. Several are the examples, including conversion of seawater or wastewater into electricity (pressure-retarded osmosis and reverse electrodialysis), energy storage for renewable energy sources such as solar or wind or direct participation into energy production processes (biofuels) [7]. The next paragraphs will explain in detail the relationship existing between membrane technology and the production of biofuels.

1.2.1 BIOFUELS

A biofuel is a fuel that is produced through contemporary biological processes, such as agriculture and anaerobic digestion, rather than a fuel produced by geological processes such as those involved in the formation of fossil fuels, such as coal and petroleum, from prehistoric biological matter. Biofuels can derive directly from plants or indirectly from agricultural, commercial, domestic, and/or industrial wastes. Biofuels are in theory carbon-neutral because the carbon dioxide that is absorbed by the plants is equal to the carbon dioxide that is released when the fuel is burned. However, in practice, whether or not a biofuel is carbon-neutral also depends greatly on whether the land which is used to grow the biofuel precursors needed to be cleared of carbon-holding vegetation or not.

Biofuels are classified in four different generations:

- *First Generation*: biofuels made from food crops grown on arable land. With this biofuel production generation, food crops are thus explicitly grown for fuel production, and not anything else. The sugar, starch or vegetable oil

obtained from the crops is converted into biodiesel or ethanol, using transesterification or yeast fermentation.

- *Second Generation*: also known as *advanced biofuels*, are fuels that can be manufactured from various types of non-food biomass. They are made from different feedstocks and therefore may require different technology to extract useful energy. Second generation feedstocks include lignocellulosic biomass or woody crops, agricultural residues or waste, as well as dedicated non-food energy crops grown on marginal land unsuitable for crop production.
- *Third Generation*: this kind of biofuels is produced using algae as source of energy-rich oils. These are an alternative to commonly known biofuel sources, such as corn and sugarcane. This oil-rich-algae can then be extracted from the system and processed into biofuels, with the dried remainder further reprocessed to create ethanol. The production of algae to harvest oil for biofuels has not yet been undertaken on a commercial scale, but feasibility studies have been conducted to arrive at the above yield estimation;
- *Fourth Generation*: like third generation ones, fourth generation biofuels are produced using algae as raw material with the difference that these are subjected to genetical modifications in order to improve the CO_2 capture and lipid production.

From these four generations, different kind of biofuels are produced such as Biogas, Biodiesel, Ethanol and so on.

Biofuels have advantages over fossil fuels such as:

- Easy availability from common biomass sources;
- Lower carbon dioxide emission, when considering the whole life cycle;
- Environmental friendliness;
- Biodegradability and sustainability.

The basic problems of biofuel are the large areas needed for feedstock cultivation and competition with food production (in the case of dedicated crops use).

1.2.2 MEMBRANE TECHNOLOGY IN BIOFUELS PRODUCTION AND PURIFICATION

In this paragraph it will be briefly shown how membrane technology results really important during the production of some of the most important biofuels produced and used nowadays. In particular, we will refer to the production systems of biodiesel, biogas and ethanol.

1.2.2.1 BIODIESEL

Among the available biodiesel production methods, the most common one is through a catalytic transesterification of vegetable oils or animal fats using a homogeneous acid or base catalyst in a batch reactor [8]. However, this production process bears some technical and environmental disadvantages mostly concerning the batch transesterification [9]:

- Mass transfer limitations due to the immiscibility of oil in methanol;
- High energy consumption because of long processing time, high reaction temperature and alcohol usage to obtain complete conversion;
- Large amount of wastewater produced after the purification steps.

Continuous membrane reactors are able to overcome most of the batch transesterification challenges by combination of reaction and separation into a single process.

There are two basic separation principles of membrane-based biodiesel production:

1. Based on the membrane pore size;

2. Based on the perm-selectivity of the membrane.

In the first case, a microporous membrane is used, typically a ceramic or carbon-based one. As shown in Figure 1.8, during the transesterification reaction in a membrane reactor, the large droplets of oil are not able to pass through the membrane pores. On the other hand, the produced biodiesel, which consists of fatty acid alkyl esters with small molecular sizes, is able to pass through the membrane along with alcohol, glycerol and catalyst. By removing the products from the reactor through the membrane, equilibrium of the transesterification reaction will be shifted to the product side, so conversion will be increased by overcoming the equilibrium limitation [8][9].

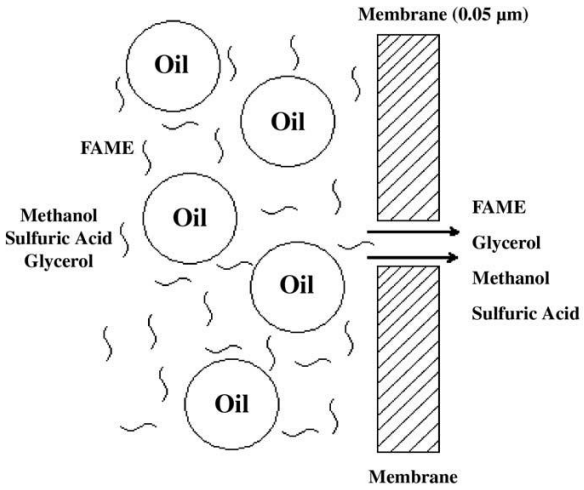

FIGURE 1.8 MICROPOROUS MEMBRANE FOR BIODIESEL PRODUCTION

According to the system based on the selectivity of the membrane, in the system based on membrane selectivity, a non-porous dense hydrophilic polymeric membrane (typically poly(vinyl alcohol)) is used [10]. The separation is based on the interaction between the target components and the membrane. Generally, glycerol and methanol experience strong interaction with –OH groups of PVA via hydrogen bonding and hence they can penetrate through the membrane. As the result, they are continuously removed from the mixture during the reaction whereas the unreacted

lipid and the product biodiesel, of which chemical structures are different with that of the membrane, are retained in the system. In such separation mechanism, the system can operate under atmospheric pressure.

1.2.2.2 BIOGAS

Biogas is produced in different environments, such as in landfills, sewage sludge and biowaste digesters during anaerobic degradation of organic material. Methane, which is the main component of biogas, is a valuable renewable energy source, but also a harmful greenhouse gas if emitted into the atmosphere. Methane, upgraded from biogas, can be used for heat and electricity production or as biofuel for vehicles to reduce environmental emissions and the use of fossil fuels [11].

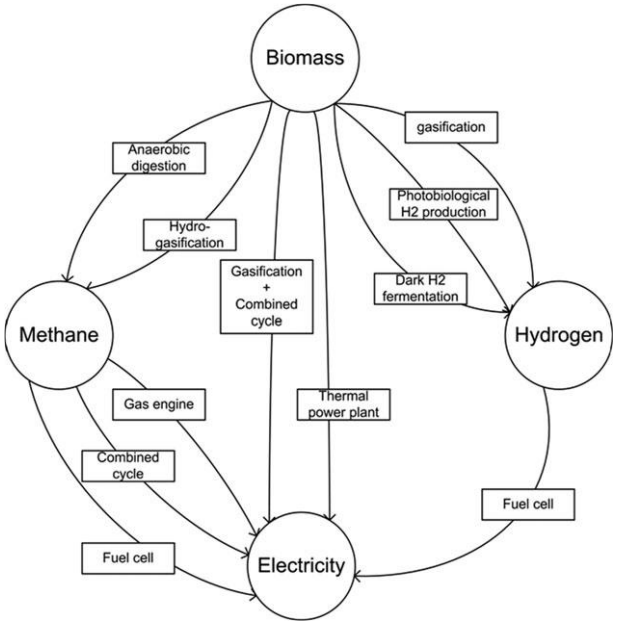

FIGURE 1.9 BIOGAS PRODUCTION PROCESS FROM BIOMASS

Depending on the plants used for biogas production, many other gases and volatiles exist in the system in trace amounts such as nitrogen, oxygen, carbon dioxide, hydrogen sulphide and other sulphuric compounds, together with other compounds

such as siloxanes, aromatic and halogenated ones. In Figure 1.10, it is possible to see the trace contents in biogas from different biogas producing plants [12].

Biogas	CH_4 (%)	CO_2 (%)	O_2 (%)	N_2 (%)	H_2S (ppm)	Benzene (mg m^{-3})	Toluene (mg m^{-3})
Landfill	47–57	37–41	<1	<1–17	36–115	0.6–2.3	1.7–5.1
Sewage digester	61–65	36–38	<1	<2	b.d.	0.1–0.3	2.8–11.8
Farm biogas plant	55–58	37–38	<1	<1–2	32–169	0.7–1.3	0.2–0.7

FIGURE 1.10 TRACE CONTENTS IN BIOGAS FROM DIFFERENT BIOGAS PRODUCING PLANTS

Even if their amount is really low compared to methane, they could have environmental impact such as stratospheric ozone depletion and reduce the quality of air. Moreover, acid gases (CO_2 and H_2S) can reduce the heating value, increase pipelines corrosion during transportation and distribution and emit sulfur dioxide in the atmosphere upon combustion.

For these reasons they must be removed and membrane technology is gaining great importance is this field. More precisely, two kinds of membranes are the mostly studied in this sector [7]:

- *Polymeric Membranes*: this kind of membranes has shown great advantages over ceramic membranes for separation processes at temperatures below 150 °C. Continuous attempts are still being made to improve their performance above all following two different approaches: chemical modification with the aim of increasing permeability without causing a lack in selectivity or cross-linking to improve selectivity of highly permeable membranes;

- *Mixed Matrix Membranes (MMMs)*: these membranes consist of organic polymer and inorganic particle phases, as shown schematically in Figure 1.11. The bulk phase (phase A) is typically a polymer; the dispersed phase (phase B) represents the inorganic particles, which can be zeolite, carbon molecular sieves, or nano-sized particles [13].

FIGURE 1.11 STRUCTURE OF A MIXED MATRIX MEMBRANE

MMMs have the potential to achieve higher selectivity, permeability or both relatively to the existing polymeric membranes, resulting from the addition of the inorganic particles with their inherent superior separation characteristics. At the same time, the fragility inherent to the inorganic membranes may be avoided by using a flexible polymer as the continuous matrix.

1.2.2.3 BIOETHANOL

Bioethanol has been identified as the mostly used biofuel worldwide since it significantly contributes to the reduction of crude oil consumption and environmental pollution. It can be produced from various types of feedstocks such as sucrose, starch, lignocellulosic and algal biomass through fermentation process by microorganisms. Depending on the origin of the biomass used for producing ethanol, it can be classified into three generation as shown in Figure 1.12.

Generation	Biomass source	Current status	Challenges
1st	Sugar and starch crops	-Technically mature -Commercially available	-The profitability heavily depends on the prices of both fossil oil and the commodity feedstock. -Compete with food prices -The greenhouse gas benefits depend on the feedstock and process used.
2nd	Lignocellulosic biomass such as agricultural wastes (e.g. straw) and energy crops (e.g. Miscanthus, poplar)	-Advanced stage of development and deployment -Demonstration stage	-Cost reduction -Availability of comparatively low-cost and sustainable feedstock
3rd	Algae	-Earlier stage of research and development	-Cost reduction -Technical challenges

FIGURE 1.12 DIFFERENT BIOETHANOL GENERATIONS

Ethanol production process is generally composed by three major steps [14]:

- Conversion of the raw material into a solution containing fermentable sugars;
- Conversion of sugars to ethanol through fermentation;
- Ethanol separation and purification

Over time, membrane technology has gained increasing importance in each of the bioethanol production steps. In Figure 1.13 is reported an overview of the three bioethanol generations production processes with potential membrane applications [15].

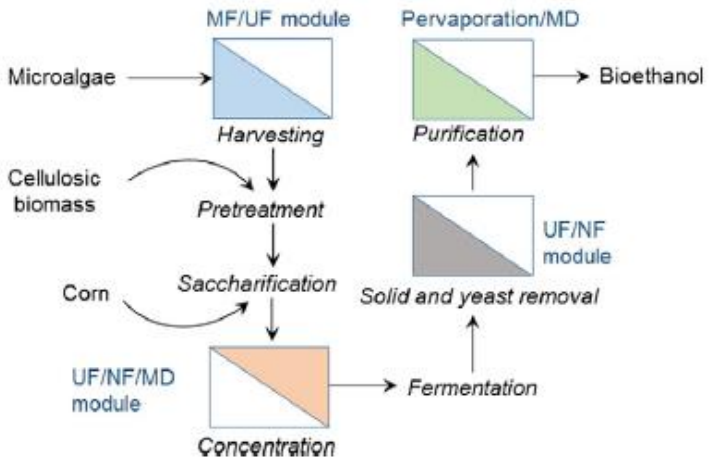

FIGURE 1.13 OVERVIEW OF THE THREE GENERATIONS BIOETHANOL PRODUCTION PROCESSES

As it is possible to see, the first potential membrane application is the harvesting of microalgae for third generation bioethanol synthesis. Microalgae cells have a very small harvesting cycle compared to other feedstocks and thus provide enough supplies to meet ethanol production demands. However, algal biomass harvesting is a challenge because of the small size of algal cells (3–30 mm in diameter), their density similar to water and the large volumes of water that must be handled to recover the biomass. MF and UF have been proven to be effective to harvest microalgae. Membranes prepared from different materials could provide variable harvesting

performance, but there is no criterion regarding the choice of membrane material for microalgae harvesting. According to the studies performed by *Rossi et al.* [16], hydrophilic membranes seemed more efficient than the others in terms of steady-state permeation flux. Furthermore, such membranes were easier to clean, partly because the negative charge decreased membrane fouling and cake formation, which represent the majority of the total resistance.

Every bioethanol generation will go through the process of saccharification and fermentation. However, for the second and third bioethanol generations based on biomass, the simple sugar concentration is often low due to the different pretreatment processes and hydrolysis efficiency. Moreover, pretreatment processes led to the formation of fermentation inhibitors that will defect the fermentation process. These problems lead to low ethanol concentrations, which in turn leads to high operational cost and energy consumption for subsequent purification steps. Membranes technology can solve these two issues also leading to a capital investment lower than the conventional methods such as evaporation. In particular, besides conventional filtration techniques (UF and NF), membrane distillation resulted to be one of the best [17]. It is a thermally driven separation process in which a microporous hydrophobic membrane acts as a physical support to separate a warm solution containing either a liquid or a gas mixture. In Figure 1.14 a schematic diagram of membrane distillation is shown.

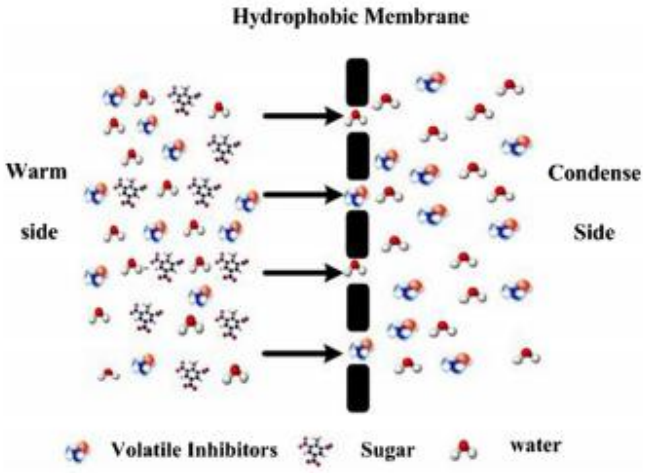

FIGURA 1.14 SCHEMATIC DIAGRAM OF MEMBRANE DISTILLATION

The last step of bioethanol production is called *Recovery* and consists in its separation and purification. The conventional method to remove and concentrate ethanol is distillation. However, this kind of procedure is affected by different limitations:

- The energy required for the process significantly increases with lower ethanol concentrations;
- Ethanol–water forms an azeotrope at 95.6 wt% ethanol. Higher concentrations of ethanol cannot be obtained through simple distillation;
- This process usually operates at high temperatures that could cause the deactivation of proteins and enzymes useful for the fermentation.

For these reasons, the use of membrane technology is a good choice in order to save Energy and costs in ethanol production. Pervaporation, described in *paragraph 1.1.1*, is the most studied membrane technique for ethanol recovery from dilute fermentation broths.

1.3 GRAPHENE-OXIDE MEMBRANES

Graphene-Oxide (GO) is an atomic sheet of graphite decorated by several oxygenated functional groups on its basal planes and at its edges, resulting in a hybrid structure comprising a mixture of sp^2 and sp^3 hybridized carbon atoms [18]. GO has several standalone applications in various fields such as optoelectronics, supercapacitors, memory devices, composite materials, photocatalysis and as a drug delivery agent. Moreover, it has shown great potential for membrane technology. As a matter of fact, GO nanosheets offer an encouraging opportunity to assemble a brand new class of ultrathin, high-flux and energy-efficient sieving membranes because of its unique two-dimensional and mono-atom-thick structure, outstanding mechanical strength and good flexibility as well as its facile and large-scale production in solution.

This has drawn the attention of researchers to explore the properties of GO nanosheets. Most of the outstanding properties of GO arise from its hybrid electronic structure as it contains both the conducting π states from the sp^2 carbon domains and also the σ states from the sp^3 carbon domains. Tuning the sp^2/sp^3 ratios of the carbon atoms, basically varying the oxidation degree using suitable chemical reactions, it is possible to modify its properties and provide novel ones that can be useful for making several improvements in the development of graphene based research applications.

1.3.1 GO STRUCTURE

GO's properties depend on its chemical structure which is closely linked to the synthesis process. Its structure basically preserves the mother structure of graphite, but has several oxygenated functional groups such as hydroxyls, epoxides and carboxyls produced during the synthesis process. Compared to graphite, due to the sterical encumbrance of these oxygenated groups, GO shows a higher inter-layer spacing than normal graphite, as it is possible to see looking at Figure 1.15. This value is around 6 Å for GO and around 3,5 Å for graphite [2].

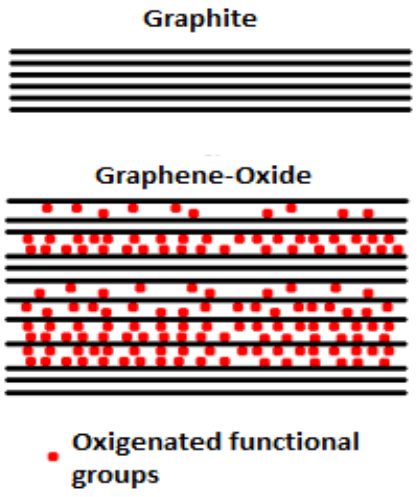

FIGURE 1.15 COMPARISON BETWEEN GRAPHITE AND GO NANOSHEETS

However, structural determination of GO is still object of discussions which have led over the years to the development of different structural models [19], from the first ones proposed by Hoffman & Holst, Reuss, Sholz-Boehm and Nakajima-Matsuo, up to the most recent one proposed by Lerf-Klinowski. This last one, shown in Figure 1.16 with the previous structural models, is the accepted and mostly widespread one.

According to Lerf-Klinowski model, two different regions can be identified:

- A poorly functionalized zone with a predominance of carbon atoms hybridized sp^2;
- A zone with large predominance of oxygenated carbon atoms hybridized sp^3

Hydroxyl and epoxy groups and their arrangement on the basal plane of GO sheet, according to this model, provides for their grouping on *islands* between the less oxidized areas, while carboxyl groups results to be poisitioned at the edge of the plane. Moreover, it is possible to observe the presence of cavities due to the formation of CO and CO_2 during the oxidation and exfoliation process of graphite.

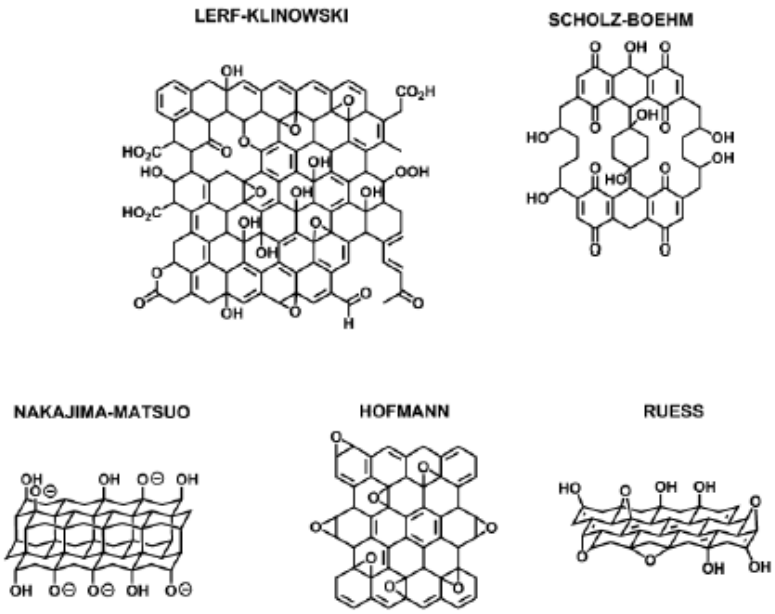

FIGURE 1.16 DIFFERENT GO STRUCTURAL MODELS

1.3.2 GO SYNTHESIS

The synthetic process of GO mainly contains two steps: oxidation of graphite and exfoliation of graphite oxide, as shown in Figure 1.17.

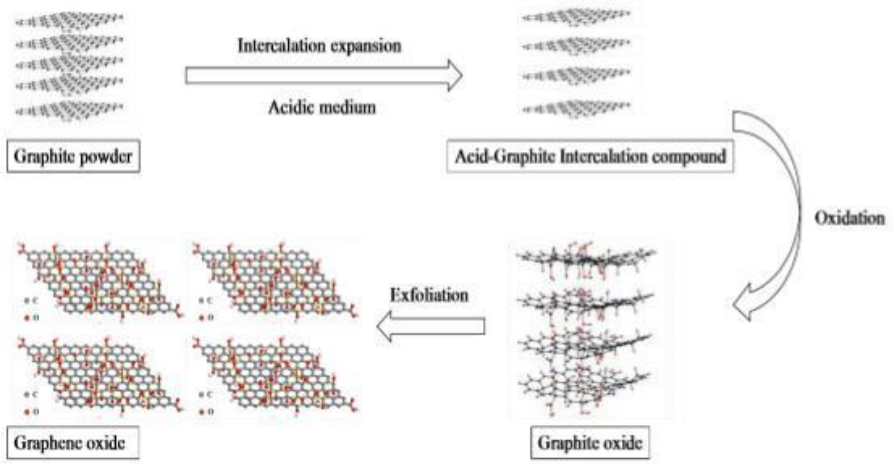

FIGURE 1.17 GO SYNTHETIC PROCESS

So far, various methods have been developed for the preparation of GO. These methods, as well as their characteristics, are summarized in Figure 1.18 [2].

Oxidant	Method	Acid	Reaction Time	Interlayer Spacing	C:O Ratio	Note
$KClO_3$	Brodie	HNO_3	3–4 days	5.95 Å	2.16	Toxic gas ClO_2
	Staudenmaier	HNO_3, H_2SO_4	1–10 days	6.23 Å	1.85	Toxic gas ClO_2, NO_x
	Hofmann	HNO_3, H_2SO_4	4 days	–	–	Toxic gas ClO_2, NO_x
$KMnO_4$	Hummers	$NaNO_3$, H_2SO_4	≈2 h	6.67 Å	2.25	Toxic gas NO_x, Mn^{2+} in GO
	Modified Hummers	$K_2S_2O_8$, P_2O_5, H_2SO_4	8 h	6.9 Å	2.3	–
	Improved Hummers	9:1 H_2SO_4/H_3PO_4	≈12 h	9.3 Å	–	Mn^{2+} in GO
K_2FeO_4	Iron-based green method	H_2SO_4	1 h	9.0 Å	2.2	Fe^{3+} in GO

FIGURE 1.18 DIFFERENT METHODS OF PRODUCTION OF GO

GO was first synthesized by Brodie in 1859 [20]. In that procedure, graphite was repeatedly oxidized in a fuming nitric acid (HNO_3) with potassium chlorate ($KClO_3$) as the oxidant for three to four days. This procedure proved to be time consuming and generated toxic gas (ClO_2), which was unsafe and harmful to the environment.
Nearly 40 years later in 1898, Staudenmaier improved Brodie's method by adding $KClO_3$ in multiple aliquots during the oxidation course and further acidifying the mixture by adding concentrated sulfuric acid (H_2SO_4). This method was more practical and convenient for the production of GO with comparable oxidation degree to Brodie's method. However, similarly to Brodie's method, this method also produced toxic gases and was not environmentally friendly.
In 1937, Hofmann modified Brodie's method, which substituted fuming HNO_3 with non-fuming HNO_3 during the oxidation course.

In 1958, a different approach was put forward by Hummers and Offeman, who utilized potassium permanganate ($KMnO_4$) as oxidant combined with a mixture of concentrated H_2SO4 and sodium nitrate ($NaNO_3$) [21]. A more highly oxygenated form of GO could be obtained by this method in less than 2 h. As such, this procedure was more efficient and less time consuming compared to the aforementioned methods and widely used in current research.
In 1999, *Kovtyukhova et al.* [22] developed a modified Hummers' method, which included two oxidation procedures. First, they preoxydized the graphite in a mixing solution of concentrated H_2SO_4, $K_2S_2O_8$, and P_2O_5 at 80 °C. After that, the mixture was further oxidized by Hummers' method. Compared to Hummers' method, the oxidization extent of graphite was slightly higher via this method. However, it should be noted that both Hummers' method and modified Hummers' method generated toxic gases and much more attention should be paid to control the reaction temperature during the process.
With the aim of developing a safer and more ecological method, *Marcano et al.* [23] proposed an improved Hummers' method in 2010, in which a mixture of H_2SO_4/H_3PO_4 with volume ratio of 9:1 was used as the mixed acid and $KMnO_4$ was used as the strong oxidant. Compared to Hummers' method, the improved Hummers'

method was simpler and higher yielding, and generated no toxic gas, making it possible for large-scale production of GO.

However, the big problem related to the Hummer's methods just described, consists in the introduction of environmentally hazardous heavy metal Mn^{2+} in the preparation process that would affect the physicochemical properties of GO. In order to solve this problem, *Gao et al.* [24] reported a new environmentally-friendly approach, in which the K_2FeO_4 was utilized as the strong oxidant to avoid the introduction of Mn^{2+}. Meanwhile, this procedure was less time consuming (1 hour) and enabled the recycle of H_2SO_4, which decreased the pollution of the environment.

In conclusion, it should be noted that the resultant GO produced with different methods differs significantly in structure and physicochemical property, which depends not only on the species and dosage of oxidant, but also on the reaction condition and initial graphite source.

1.3.3 GO CHARACTERIZATION

In order to verify the successful synthesis of GO and identify its chemical structure, a variety of characterization techniques have been employed. A short detailed description of the techniques used for the GO characterization is shown in Figure 1.19

Name	Characterization Method	Characterization Information
Micromorphology and size of GO	SEM	Lateral size distribution of GO sheets, observe the structural morphology of GO
	TEM	Morphology of GO (wrinkles), monolayer character of GO sheets
	AFM	Lateral size and thickness of GO sheets
Thermal stability	TGA	Thermal stability of GO
Chemical structure of GO	XPS	Quantitatively analyze the chemistry composition of GO
	ICP-MS	Chemistry composition of GO, identified the metal ion content in GO
	FTIR	Characteristic bands corresponding to oxygen functional groups, confirmed the successful synthesis of GO
	XRD	Crystalline structures of the GO nanosheets, inter-sheet distance of GO, confirmed the successful synthesis of GO
	Raman spectroscopy	Analyze the chemical structure of GO combined with XPS, FTIR, XRD, ICP-MS
Electrochemical property	Zeta potential measurement	GO nanosheets are negatively charged over a wide pH range

FIGURE 1.19 GO CHARACTERIZATION METHODS

SEM and TEM are the most used techniques in order to analyze the micromorphology and structure of GO. In Figure 1.20 two examples of the images obtained using these two techniques are reported [1].

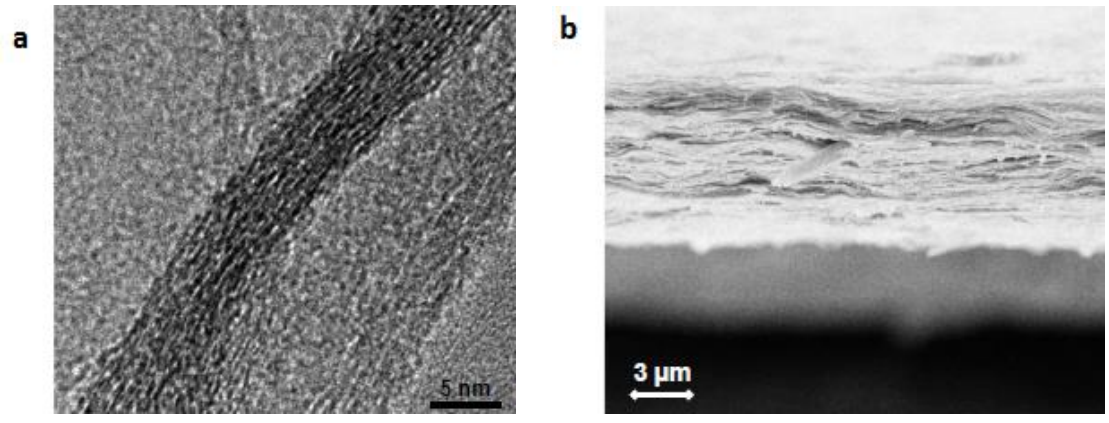

FIGURE 1.20 (A) TEM AND (B) SEM IMAGES OF GO

In addiction, other two techniques are used in order to study the chemical structure of GO are:

- *X-Ray Diffraction*: the XRD curve of GO measured with a Cu X-Ray source shows a narrow and intense peak around a value of 2Theta of 13°. This peak is related to the interlayer d-spacing of the plan (002). Sometimes, It is also possible to identify a second peak positioned to a 2Theta value of 25° corresponding to the planes (110) and produced by GO inter-plane reflections. An example of XRD of GO is shown in Figure 1.21 [25];

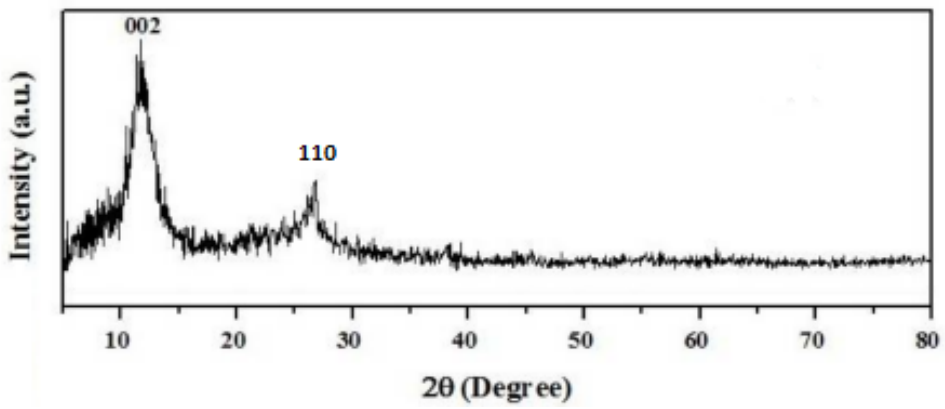

FIGURE 1.21 DIFFRACTOGRAM OF GO

- *Raman Spectroscopy*: the Raman spectra of graphitic compounds are identified by two main peaks located approximately at 1350 cm^{-1} (peak G), corresponding to the absorption of sp^2 carbons, and 1600 cm^{-1} (peak D), generated by the absorption of sp^3 carbons. Therefore, the Raman spectra of pure graphite, characterized by the presence of only sp^2, only show the G peak. For GO, as a consequence of the introduction of oxygenated functional groups with consequent formation of sp^3 carbons, the appereance of the D peak is observed. An interesting parameter for the characterization of GO derives from the analysis of the intensity ratio between the D and G peaks. An increase of this ratio is index of an increase of the oxidation degree of graphite.

According to the literature [26], a ratio I_D/I_G of around 0,90 is symbol of an optimal oxidation degree of GO.

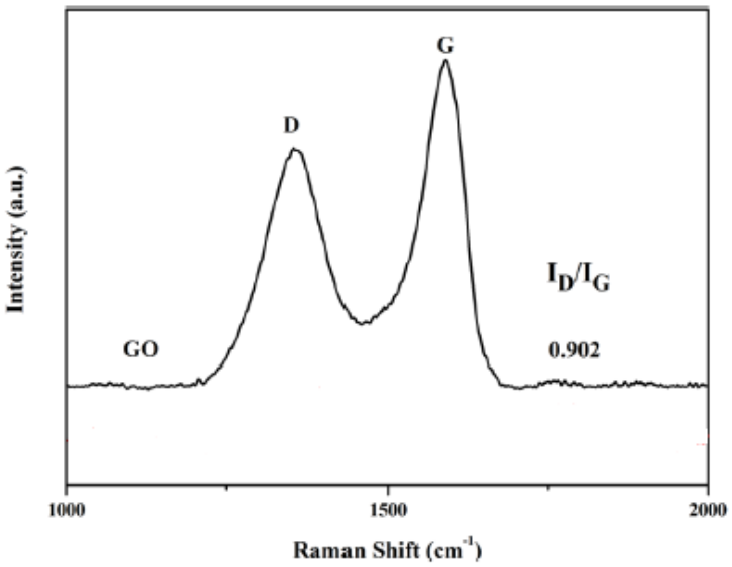

FIGURE 1.22 RAMAN SPECTRUM OF GO

To obtain more information about GO properties, TGA and Zeta potential are also employed by researchers to judge its thermal stability and electrochemical properties.

1.3.4 GO-BASED MEMBRANES

Today, there is a blossoming of studies focused on the development of GO-based membranes, including:

- *Free-standing GO membranes*: GO membrane is directly used as a separation layer;
- *Supported-GO membranes*: GO membrane is supported by a polymeric or an inorganic substrate with GO layer as the active separation layer;

- *GO-modified composite membranes*: the GO-based membranes are obtained by directly incorporating GO nanosheets into a polymer casting solutions during membrane fabrication process or functionalizing membrane surface by post-coating of the pre-fabricated membrane with GO nanosheets

In the next paragraph the possible fabrication methods for supported-GO membranes will be described as they are relevant to this project.

1.3.4.1 PREPARATION OF SUPPORTED GO MEMBRANES

Although free-standing GO membranes have achieved great progresses in membrane separation applications, a GO membrane supported on mechanically stable support for high-pressure application is rather necessary. Additionally, depositing GO layers onto certain polymeric or inorganic membrane surface could also improve the separation performance and antifouling property of pristine membranes.

Chu et al. [27] prepared GO-coated PES UF membranes via a simple vacuum filtration process, as shown in Figure 1.23, and used the resultant membranes for humic acid (HA) removal. The results showed that the GO-coated membranes presented approximately 20% higher pure water flux and 3.4 times higher HA rejection than that of the original PES membranes. Meanwhile, they reported that GO sheets were not easily damaged or detached from the PES substrate during filtration or water rinsing due to the strong hydrogen bonding interactions between the sulphone groups on PES and carboxylic groups on GO sheets.

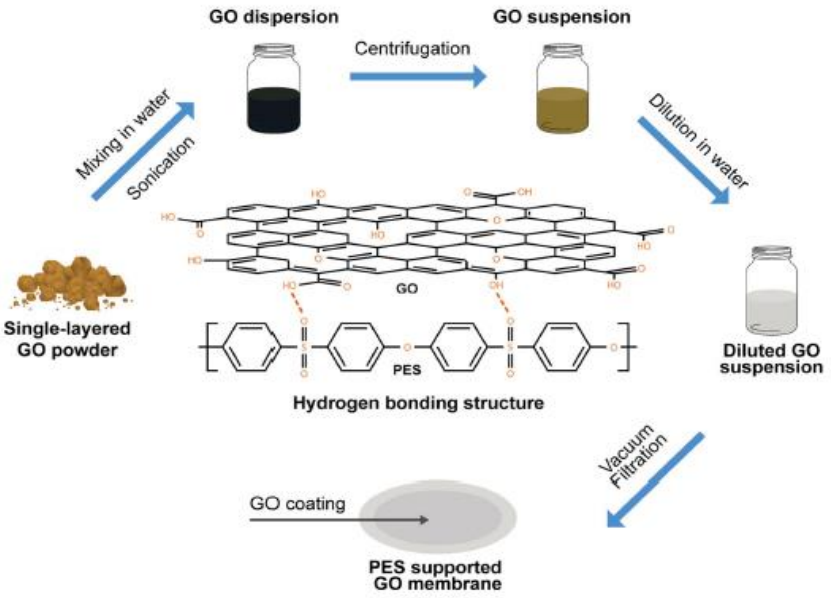

FIGURE 1.23 GO-COATED PES ULTRAFILTRATION MEMBRANE VIA VACUUM FILTRATION PROCESS

The methods developed for GO-based membrane production are different. More precisely, all the possible techniques can be classified in three groups, as shown in Figure 1.24:

- *Filtration-assisted Method*s: including vacuum filtration and pressure-assisted filtration. It is a widely used approach to prepare GO membranes at present, especially for the free-standing GO membranes. This method allows reasonable and easy control over the membrane thickness and microstructure, and is a potential route for large-scale preparation of GO membrane;

- *Casting/coating-based Methods*: these methods basically consists in the deposition of the GO solution on a polymeric support followed by the evaporation of water. This last step can be forced introducing dry nitrogen. These techniques result to be suitable for large-scale production of continuous GO membranes; the only problem is the poor control over the membrane thickness;

- *Layer-by-Layer (LbL) Method*: Recently, LbL assembly approach has been attracting great attention for the preparation of GO membranes. An interlayer stabilizing force can be conveniently introduced into laminate GO membranes by electrostatic interaction or covalent bonding through this method. This method leads to an easy control of the GO layer number and thickness.

Method	Description	Note
Filtration-assisted	Vacuum filtration Pressure filtration	Good nanoscale control over the membrane thickness; laminar structure of GO membranes is dictated by the filtration force; highly scalable
Casting/coating-based	Spinning-casting/coating Drop-casting Dip-coating Spray-coating Doctor blade-casting	Nonuniform deposition of GO nanosheets; poor control over the membrane thickness; producing highly continuous GO membranes; highly scalable
LbL assembly	Layer-by-layer assembly	Easily control of the GO layer number, packing, and thickness

FIGURE 1.24 GO-BASED MEMBRANE PRODUCTION METHODS

1.3.4.2 MEYER ROD COATING

A novel strategy to produce uniform GO films on a large scale directly on the surface of a substrate uses the rod-coating (*Meyer rod*) technique. Meyer rod coating is a well-known coating technique that is widely used in the coating industry for making liquid thin films in a continuous and controlled manner. A Meyer rod is a metal bar with a wire wrapped around the outside that is used to draw a solution over a substrate surface. The diameter of the wire wrapped around the bar determines the thickness of the wet coating film. This technique can be used to coat directly onto different substrates at room temperature and in a scalable way for roll-to-roll production in industry.

Actually, rod coating has been used in different studies. *Zhang et al.* [28] used this deposition technique for the production of sheath–core-structured single-fiber strain sensors using ultrafine graphite flakes obtaining sensors that exhibits a high sensitivity and outstanding stability. This technique was also used in 2010 by *Hu et al.* [29] in order to fabricate silver nanowire films and even carbon nanotube films on a large scale.

Wang et al. [30] were the first to use Meyer rod coating method for the deposition of GO on a polyethylene terephthalate (PET) substrate. Figure 1.25 shows a typical wire-wound-rod setup for the lab-scale coating.

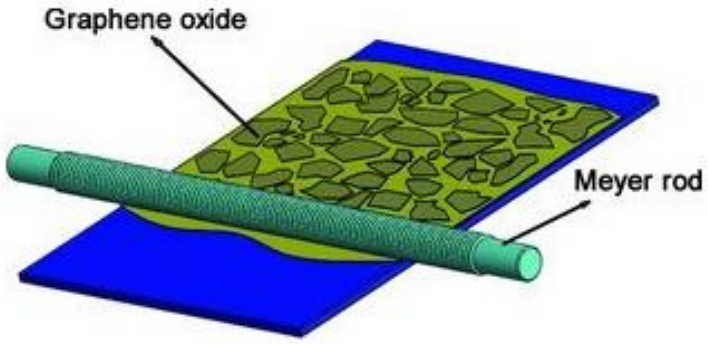

FIGURE 1.25 MEYER ROD COATING METHOD FOR GO-BASED MEMBRANES

A homogeneous GO suspension passes through the groove between the wires when the rod moves over the substrate. The initial shape of the coating is a series of stripes, spaced apart from each other according to the spacing of the wire windings. Almost immediately, the normal surface tension pulls these stripes together, forming a flat, uniform film, ready for drying in air or under heat.

Using the rod-coating method, the thickness of GO films can be precisely controlled from a single layer to tens of layers by adjusting the concentration of the GO solution

1.3.5 GO STABILIZATION

At present, despite significant advancements in GO-based membranes have been achieved, a few critical challenges in realizing real-world application of GO-based membranes still exist. Specifically, the instability of the inter-layer spacing between adjacent GO nanosheets is a great challenge for utilizing laminar GO membranes as selective aqueous separation barriers, especially for water-related treatment. This is because GO membrane easily disintegrated and redispersed in water over time due to the highly hydrophilic nature of the GO sheets and electrostatic repulsion between the negatively charged GO sheets on hydration. For this reason the integrity of the laminar GO membranes and inter-layer nanochannels formed by stacking GO sheets would be damaged during aqueous separation process. Therefore, it is very much desirable to enhance the structural stability of GO membrane by forming stable bonding between GO nanosheets to realize real-world applications of GO membranes in aqueous environment.

Currently, it has been reported that stable GO-based membranes suitable for aqueous system applications could be obtained by:

- The introduction of various cross-linking interactive forces, including electrostatic interactions and covalent bonds between adjacent GO nanosheets;
- Reduction of GO membranes

Different papers reporting possible ways to stabilize GO have been published. A highly stable GO-based ultrathin hybrid membrane was developed by *Zhao et al.* [31]. They produced a GO-based ultrathin hybrid multilayer membrane using gelatine (GE) as cross-linker and depositing it alternately with GO on a hydrolyzed polyacrylonitrile (H-PAN) UF membrane through electrostatic attractions, hydrogen bonds and hydrophobic interactions. Desirable operation stability was acquired in the long-term membrane separation experiment and synchronous enhancement in permeation flux

and separation factor for pervaporation dehydration of ethanol aqueous solution was achieved in comparison with GE/H-PAN pristine membrane.

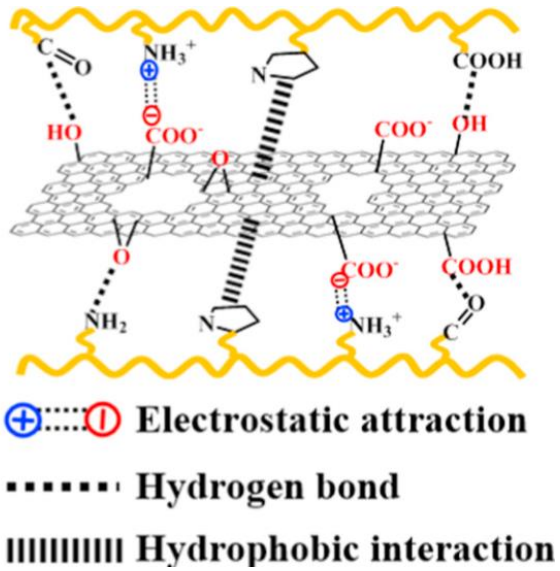

FIGURE 1.26 SCHEMATIC REPRESENTATION OF INTERFACIAL INTERACTIONS IN *ZHAO et al.* MEMBRANE

Boffa et al. [1] used a humic acid-like biopolymer (HAL), extracted from compost with a yield of ~20%, to fabricate composite GO-HAL membranes. The HAL brings a high degree of disorder to the membrane structure, with the benefit of an increased water permeation rate. Upon thermal stabilization, the membrane with higher biopolymer loading presented an ideal water/ethanol selectivity and a water permeance higher than the pristine graphene oxide membrane.

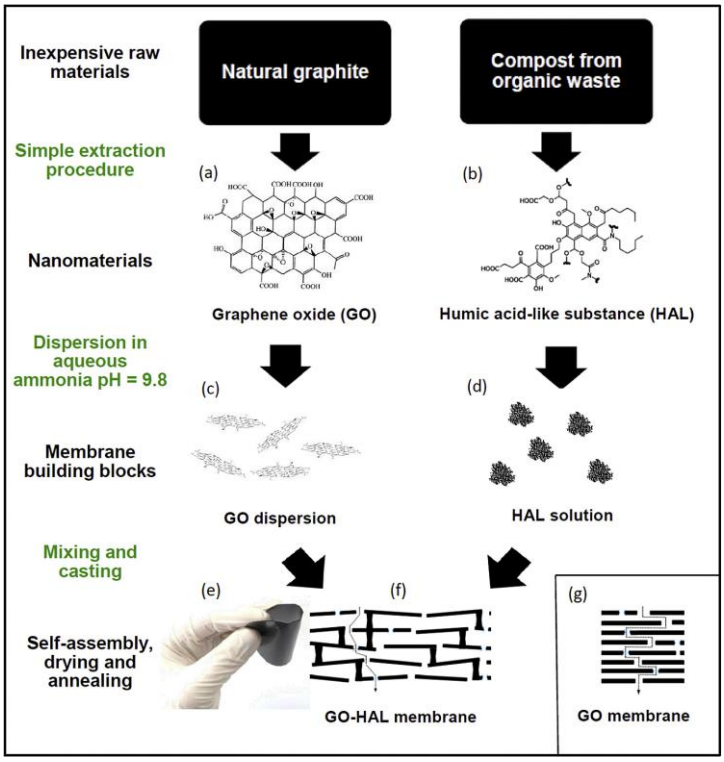

FIGURE 1.27 GO-HAL MEMBRANE PRODUCED BY *BOFFA et al.*

Some studies also showed that reducing GO sheets might also increase the stability of GO membrane by enhancing the π-π interactions between the GO nanosheets. *Yang et al.* [32] fabricated an adhesive polydopamine-coated reduced GO (PDA–rGO) membranes by chemically reducing GO laminates and then introducing a PDA layer onto the rGO laminates and used for Forward Osmosis (FO) desalination. rGO laminates sustainably retained their compacted nanochannels compared to pristine GO laminates, which increased the selectivity of hydrated ions. In addition, adding a PDA coated onto the rGO laminates improved the hydrophilicity of the rGO laminate surface, which accelerated the water absorption speed.

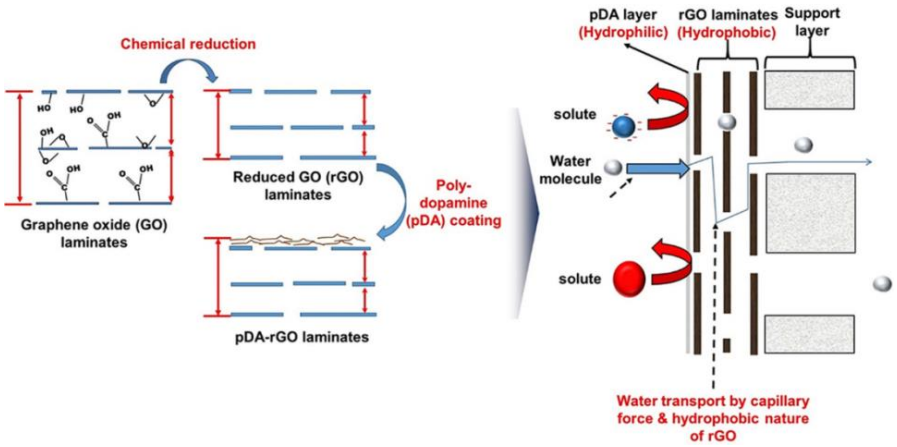

FIGURE 1.28 PDA-rGO MEMBRANE PRODUCED BY *YANG et al.*

2. EXPERIMENTAL SECTION

2.1 MATERIALS

- The hyperbranched polyol (HBPO), viz. hyperbranched bis-MPA polyester-16-hydroxyl, generation 2, molecular weight 1749.79 (97%), sodium nitrate (> 99% purity), potassium permanganate (> 99% purity) and hydrogen peroxide (30% w/w in water) were obtained from Aldrich (97%);

- Polyethylene Glycol with different molecular weights were obtained from Fluka.

- Polyethersulphone membrane (molecular weight cutoff 100,000 Da) was supplied by Synder Filtration;

- Graphene oxide (GO) dispersions were prepared from natural graphite (Graphit Kropfm¨uhl GmbH) as described in the next paragraph [33];

- Humic Acid-like substance (HAL), was extracted from Compost Florawiva (Acea Pinerolese Industriale).

2.2 GRAPHENE-OXIDE (GO)

2.2.1 SYNTHESIS

GO was produced following the Hummer's Method process. According to this method, Potassium Permanganate ($KMnO_4$), Sulfuric Acid (H_2SO_4) and Sodium Nitrate ($NaNO_3$) are used in the oxidation process, while Hydrogen Peroxide (H_2O_2) was used for the exfoliation of Graphite-Oxide [2].

Hummers's Method process is composed by several number of steps which are described in the following:

1. 2 g of graphite and 2 g of $NaNO_3$ are weighted and placed in a beaker with 92ml of H_2SO_4, all put under stirring for about ten minutes in an ice bath;
2. 12 g of $KMnO_4$ are weighted and added really slowly to the solution. Then, the ice bath is removed and the solution is put in a water bath at 35 °C for 1 hour. After this, the solution is put in an oil bath for other 30 minutes at 90 °C. Then, the solution is removed from the oil bath and put under stirring at room temperature since it's cooled;
3. 160 ml of distilled water (DI) are slowly added to the solution, keeping it under stirring for one hour. The color of the solution changes from green-black to golden brown;
4. Other 400 ml of DI water are added at the solution in order to stop the oxidation reaction. Graphite-Oxide is so produced;
5. 12 ml of H_2O_2 are added to the suspension in order to exfoliate graphite-oxide and obtain Graphene-Oxide. The color of the suspension become golden yellow as shown in Figure 2.1;
6. The pH of the suspension obtained at this point is really low (around 2-3); for this reason, it is washed several time with DI water and centrifuged each time since the pH becomes almost neutral (around 6);

7. As soon as the neutral pH has reached, the GO suspension obtained is freezed in liquid nitrogen and put in a vacuum system for two days. The final product is shown in Figure 2.2

FIGURE 2.1 GAPHENE-OXIDE SUSPENSION

FIGURE 2.2 FINAL PRODUCT AFTER DRYNG PROCESS

2.2.2 CHARACTERIZATION

In order to understand if the synthesis of GO was successful, the product was analyzed using XRD and Raman Spectroscopy. These two kinds of analysis are extremely useful when used together to understand if the synthesis process of GO led to the desired result. If the results obtained by both the analysis are positive, it means that the synthesis process of GO has occurred. In the two following paragraphs these two techniques will be briefly described.

2.2.2.1 X-RAY DIFFRACTION (XRD)

X-Ray Diffraction (XRD) is a technique that allows to study the interaction between an X-ray beam and the analyzed sample. More precisely, X-ray diffraction is the elastic

scattering of x-ray photons by atoms in a periodic lattice. The scattered monochromatic x-rays that are in phase give constructive interference. Figure 2.3 illustrates how diffraction of x-rays by crystal planes allows to derive lattice spacings by using the Bragg's law

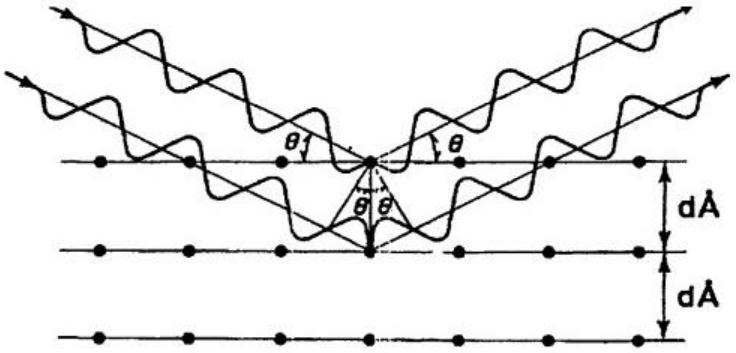

FIGURE 2.3 INTERACTION BETWEEN X-RAYS AND LATTICE

$$n\lambda = 2d \sin \theta$$

where n is an integer called the order of reflection, λ is the wavelength of x-rays, d is the characteristic spacing between the crystal planes of a given specimen and θ is the angle between the incident beam and the normal to the reflecting lattice plane. By measuring the angles θ, under which the constructively interfering x-rays leave the crystal, the inter-planar spacings d of every single crystallographic phase can be determined.

XRD analysis of the samples were recorded on a PANalytical empyrean X-ray diffractometer with Cu Kα (λ = 1.5406 Å) radiation in a 2θ range of 5-30°.

2.2.2.2 RAMAN SPECTROSCOPY

In Raman Spectroscopy the radiation emitted by a laser source interacts with the roto-vibrational motions of the molecules with the consequent re-emission of light at different wavelengths from that of the incident radiation. The Raman spectrum obtained thus provides a digital fingerprint of the studied compound allowing its identification.

Raman Spectroscopy is a really advantageous technique: it is non-destructive, highly sensitive and provides several information, both structural and electronic, of the examined compound; as a matter of fact, the information that can be derived from a single spectrum are:

- The peak intensity gives information about the quantity of a specific compound;
- A peak shift can identify stress and strain states;
- The peak width reveals the degree of crystallinity;
- The polarization state provides information regarding crystal symmetry and orientation

Moreover, it is a really fast analysis and can be performed on a variety of samples such as gases, liquids, powders and solids (only fluorescent materials can cause problems, whereas pure metals are Raman-inactive). In general, there is no sample preparation required and Raman spectroscopic measurements can be performed in situ, in vitro, and in vivo. The maximum applicable sample size for Raman imaging is dependent on the Raman microscope capabilities and the maximum scan range is dependent on the integrated scan stage. Typically, sample areas from μm^2 up to mm^2 can be investigated.

It has now become a basic standard technique for the identification and characterization of all the components of the carbon family, including graphene and its derivatives, like GO.

2.3 PREPARATION OF FREE-STANDING CROSS-LINKED GO FILMS

For the stabilization of GO, three different materials were used as cross-linkers. Each of them was used in different amounts, always using the same amount of GO, in order to understand the effects on the structure and stability of the free-standing films produced. It was used:

- Polyethylene Glycol (PEG);
- A synthetic hyperbranched polyol (HBPO);
- Humic Acid-like substances, derived from urban waste (HAL)

In the table below (Table 2.1), the different concentrations for each cross-linker used for stabilized GO are reported:

	K PEG:GO (meq/g)
PEG 200-600-2000 g/mol	5
	10
	20
	50

	K HBPO:GO (mg/mg)
HBPO	0.01
	0.05
	0.1
	0.2

	K HAL:GO (mg/mg)
HAL	0.01
	0.05
	0.1
	0.2
	0.4

TABLE 2.1 CROSS-LINKERS-GO RATIOS USED FOR THE PRODUCTION OF FREE-STANDING FILMS

The cross-linking reaction is carried out as follow:

1. 100 mg of GO are dissolved in DI by stirring for 1 hour;
2. The required amount of cross-linker is dissolved in DI by stirring for 12 hours (for HBPO, 2 ml of dimethyl formamide is used as co-solvent);

3. The suspensions of GO and cross-linker are mixed, such that the final concentration of GO is 2 mg/ml, 100 µl of concentrated HCl are added to the suspensions and it is allowed to stir for a further 4 hours for the cross-linking process to progress;
4. The suspension is then centrifuged at 12500 rpm for 20 minutes and the supernatant is discarded;
5. The solid thus obtained is coated onto a polyethylene surface and left to dry for 12 hours;
6. Thereafter, the cross-linked GO film is lifted off from the polyethylene surface and dried in an oven at 80 °C for 24 hours.

The final product is shown in Figure 2.6.

FIGURE 2.4 FREE-STANDING CROSS-LINKED GO FILMS

The cross-linked films are then analyzed by X-Ray Diffraction (XRD) technique in order to understand if the cross-linking reaction occurred. If the d-space of the cross-linked film is higher than that of the pure GO film, it means that the cross-linker intercalated between the GO layers and that the cross-linking reaction was successful.

XRD analysis of the free-standing films samples were recorded on a PANalytical empyrean X-ray diffractometer with Cu Kα (λ = 1.5406 Å) radiation in a 2θ range of 5-30°.

2.4 STABILITY STUDIES

As it was said previously, the most serious problem about GO is its instability in water due to the highly hydrophilic nature of the GO sheets and electrostatic repulsion between the negatively charged GO sheets on hydration. This is the reason why we tried to stabilize the interacting sheets by cross-linking.
The stability test consists in putting a part of the films produced in water and tumble it for 24 hours on a laboratory rotator. After this period a series of analyses has performed in order to understand the amount of GO that each film has lost in water during this time and if some structural changes have occurred.
The free-standing films were submerged in DI water, such that the ratio of water to film was 15 ml for 10 mg of film weight.

At the end of the test two different analyses were performed:

- To find out some structural changes caused by the water swelling, XRD analysis was carried out. The films were analyzed in two different conditions:

  - ✓ **WET CONDITION**: films are removed from water and immediatly analyzed in order to understand if they absorbed some water during the test;

  - ✓ **DRY CONDITION**: after the wetting step, the films are put in oven at 80 °C for one hour and analyzed again in order to measure the d-space

change (if the d-space value returns back to the original one, the wetting is a reversible process).

- Once analyzed the structural changes of the films using XRD, it was tried to understand the amount of GO each film could have lost in water. Several suspensions of known amounts of GO were prepared and the absorbance at 300 nm, recorded on an ultraviolet-visible spectrometer (Varian Cary 50 UV-vis Spectrophotometer), was used to obtain the calibration curve reported in Figure 2.5. Then, an aliquot of water after testing was separated and the absorbance at 300 nm used to determine the concentration of GO dispersed in water.

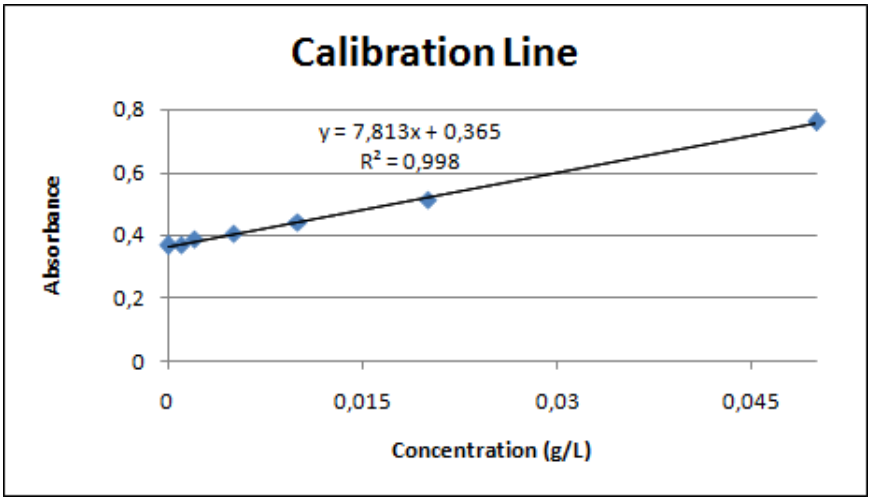

FIGURE 2.5 UV-VIS CALIBRATION LINE AND THE CONCENTRATION OF THE STANDARD SOLUTIONS USED FOR OBTAIN IT

The Lambert-Beer law was considered:

$$A = \varepsilon b C$$

Where ε is the *molar attenuation coefficient* of the attenuating species in the suspension, b is the path length of the beam of light through the material sample and C is the concentration of the attenuating species in the suspension.

2.5 PREPARATION OF LARGE-AREA SUPPORTED GO FILMS

The composition with the highest loading of cross-linker that was found to be stable in water was chosen for preparing large-area supported GO films. The cross-linking reaction is carried out as described in *paragraph 1.4*, with the difference that the final concentration of the GO before addition of the concentrated HCl was 14 mg/ml. The solution was put under stirring for 4 hours and the suspension obtained was coated according to Meyer Rod coating method on the polyethersulphone membrane, which was then dried in an oven at 80°C for 24 hours. An example of the membranes obtained is shown in Figure 2.7.

FIGURE 2.6 EXAMPLE OF A LARGE-AREA SUPPORTED GO MEMBRANE

2.6 VAPOUR PERMEATION STUDIES

Circular discs (diameter ~ 3 cm) cut from the large-area supported membranes were used to cap glass bottles, with caps screwed using silicone O-rings to ensure air-tightness. The two kinds of analysis carried out are described below.

2.6.1 DETERMINATION OF PERMEANCE OF WATER AND ETHANOL

100 ml of either water or ethanol were put in the bottles and placed in a vent oven at four different temperatures (30, 40, 50 and 60 °C). At each temperature, the reduction in weight after 6, 10 and 24 hours was noted. A bottle sealed with non-permeable aluminium foil was used as a control. Each bottle was weighed before being placed in the oven and, knowing the mass changing (Δm), it was possible to calculate the permeance (P) of each solvent through the membrane, its theoretical Activation Energy (E_a) and the ideal selectivity (α) of the membrane.

2.6.2 DEHYDRATION OF ETHANOL-WATER MISTURE

Mixtures of ethanol and water were prepared by mixing absolute ethanol with DI water, and their compositions determined by Karl Fisher titration on a C20 Mettler Toledo automatic titrator. Care was taken to ensure that the weight fraction of ethanol was less than that at the azeotropic point (i.e., 95.6 weight *per cent*). The average composition of the initial water/ethanol mixture is reported below:

% Water	% Ethanol
5.50	94.50

The mixtures were then poured into glass bottles, which were capped with membranes and sealed as described above. For each type of membrane, sets of three bottles were prepared. Vapor permeation was carried out by placing the bottles in a vent oven at 50°C for 24 h. The compositions of the retentates in the bottles were again determined by coulometric Karl Fisher titration. It was also possible to calculate the real selectivity of the membrane and compare it with the ideal one considering few simplifications described in the following.

2.6.2.1 KARL FISHER TITRATION

Karl Fisher Titration is an universally recognized method for measuring water content in all kinds of substances. The determination of water content is really important cause its presence could affect the performance of the product, its organoleptic properties and stability.

Karl Fisher's titrator follows the coulometric titration which is the most suitable for the determination of very low water content, up to a maximum of 5% (recommended value). During Karl Fisher's reaction, water reacts with iodine and sulfur dioxide, in presence of a basic substance (RN) and an alcohol.

$$H_2O + I_2 + SO_2 + CH_3OH + 3\,RN \rightarrow (RNH)SO_4CH_3 + 2(RNH)I \quad (1)$$

In coulometric titration iodine is elettrolitically generated according to the following reaction

$$2\,I^- \rightarrow I_2 + 2\,e^- \quad (2)$$

It reacts, following the reaction (1), until there is some water in the reaction cell. When all the water has reacted, an excess of iodine will be created and it will be detected by a double platinum electrode. According to Faraday's laws, the amount of iodine generated is proportional to the current produced.

According to reaction (1), I_2 and H_2O react in a 1:1 ratio, therefore one mol of water is equivalent to 2*96500 Coulomb. The total amount of water contained in the sample can thus be determined measuring the total current consumption.

In Figure 2.7 the Karl Fisher titrator used for the analysis is shown.

FIGURE 2.7 C20 METTLER TOLEDO AUTOMATIC TITRATOR

3. RESULTS AND DISCUSSION

3.1 GRAPHENE-OXIDE CHARACTERIZATION

The diffractogram obtained from the pure GO synthesized as described in *paragraph 2.2.1* is reported below.

The XRD of GO typically consists of a broad peak at 2θ of under 15° corresponding to the (002) diffraction line [1], which, using the Bragg's equation, gives an inter-layer spacing greater than 6 Å. 26,48° corresponds to a d-spacing of 3,4 Å for graphite.

As it is possible to see in Figure 3.1, the 2θ angle obtained and, therefore, the inter-layer spacing, is similar to the one reported in literature [34].

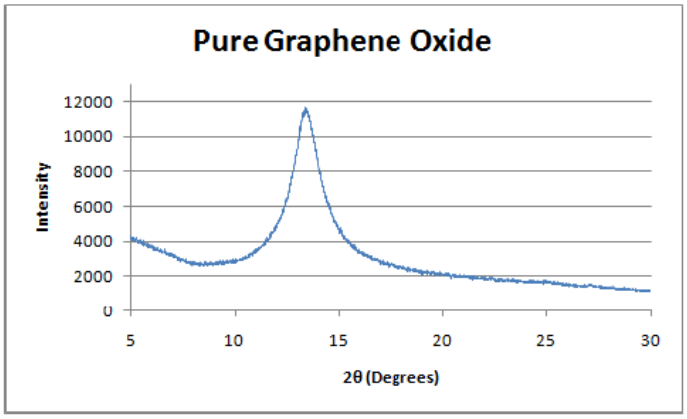

2θ	d-space (Å)
13.384	6.614

FIGURE 3.1 PURE GO DIFFRACTOGRAM

As it was said previously, this is the first step that lets us prove that the synthesis was successful.

It's possible to definitely confirm it looking at the Raman spectrum shown in Figure 3.2:

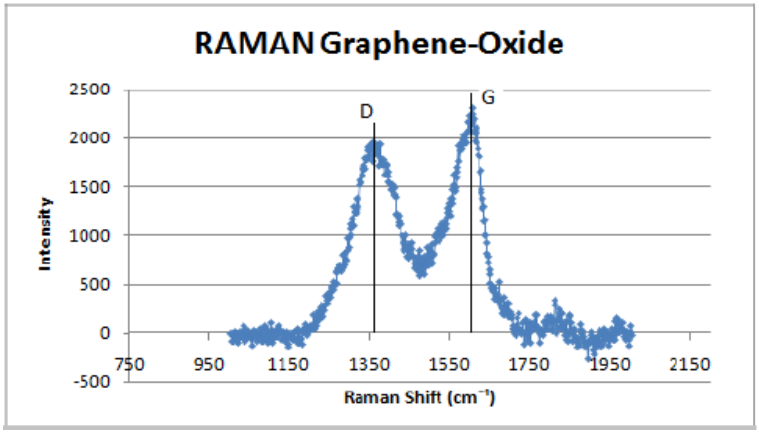

FIGURE 3.2 PURE GO RAMAN SPECTRUM

As a matter of fact, it is possible to see the D peak at ≈1360 cm^{-1} and the G peak at ≈1580 cm^{-1}. Moreover, the intensity ratio I_D/I_G obtained was 0,91, really similar to the one reported in literature and index of an optimal oxidation degree of the GO produced.

According to the results obtained through both the analyses, it was definitely possible to confirm that the synthesis process of GO was successful.

3.2 STABILIZATION OF GO WITH DIFFERENT CROSS-LINKERS

As it was said in *paragraph 2.3*, three different kind of compound, in different concentrations, were used as cross-linker species with the aim of stabilize GO:

- Polyethylene Glycol (PEG)
- A synthetic hyperbranched polyol (HBPO);
- Humic Acid-like substances, derived from urban waste (HAL).

First of all, the free-standing films produced are analyzed by XRD in order to understand if, through a change in d-space, the cross-linking reaction has occurred. In order to confirm that the cross-linking reaction produced an increase in stability of GO in water, a stability test was performed, as described in *paragraph 2.4*.

In order to have a quantitative result about the stability of GO, an aliquot was drawn out from the water and the absorbance at 300 nm was noted and used to determine the concentration of GO dissolved in water.

After the UV-vis analysis, a second XRD was performed on the swollen films in *wet conditions* and *dry conditions.*

3.2.1 POLYETHYLENE GLYCOL

Polyethylene glycol (PEG) is a white, free flowing powder or creamy white flakes used as a water soluble lubricant for rubber moulds, textile fibres and metal forming operations. It is also used in water paints, paper coatings, polishes and in the ceramic industry, as well as for chromatographic stationary phases.

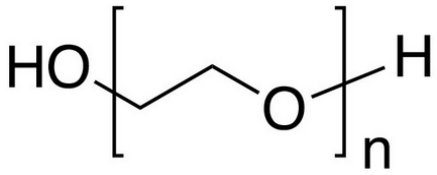

FIGURE 3.4 MOLECULAR STRUCTURE OF POLYETHYLENE GLYCOL

PEG was used in the first part of this project. Precisely, it was used in three different molecular weights in order to understand how this factor could affect the structure and stability of GO in water. PEG 200 g/mol, 600 g/mol and 2000 g/mol (in the

following PEG 200, PEG 600 AND PEG 2000, respectively) were used as possible cross-linkers and each of them was used in four different concentrations:

- 5 meq_{PEG}/g_{GO}
- 10 meq_{PEG}/g_{GO}
- 20 meq_{PEG}/g_{GO}
- 50 meq_{PEG}/g_{GO}

100 mg of GO were used for all the tests.

3.2.1.1 PEG 200

As it is possible to see looking at Figure 3.5, all the samples analyzed show a 2Theta angle lower than that of pure GO (**dashed line**). This shift, according to Bragg's Law, indicates a d-space increase confirming that an interaction between GO and the cross-linker has occurred.

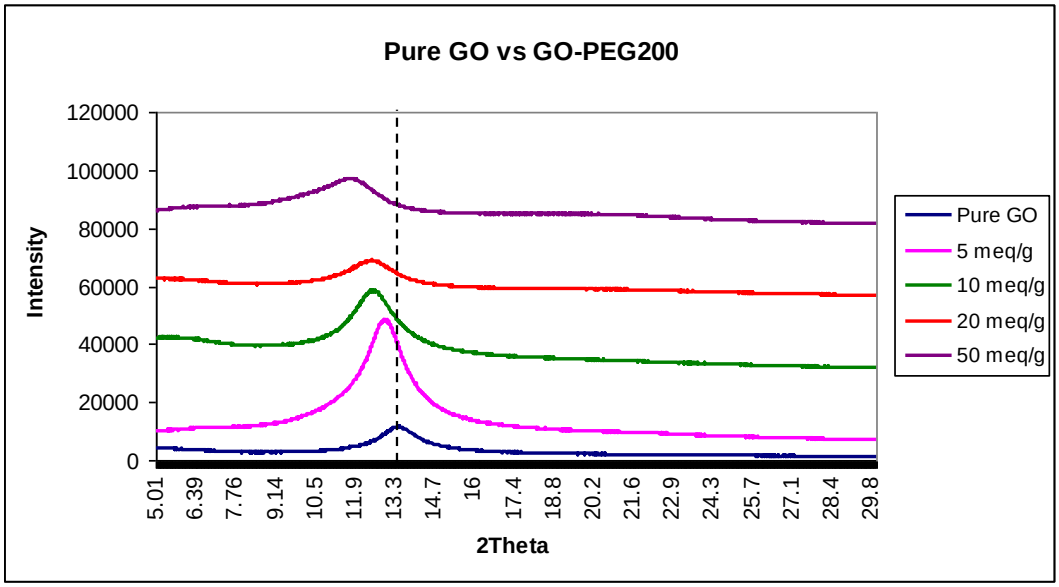

FIGURE 3.5 DIFFRACTOGRAM OF THE FREE-STANDING GO FILMS CROSS-LINKED WITH PEG 200 g/mol

Moreover, the d-space increase seems directly correlated to the amount of cross-linker used for the reaction. As a matter of fact, as shown in Figure 3.6, it is possible to see a linear increase of d-space related to a bigger amount of cross-linker.

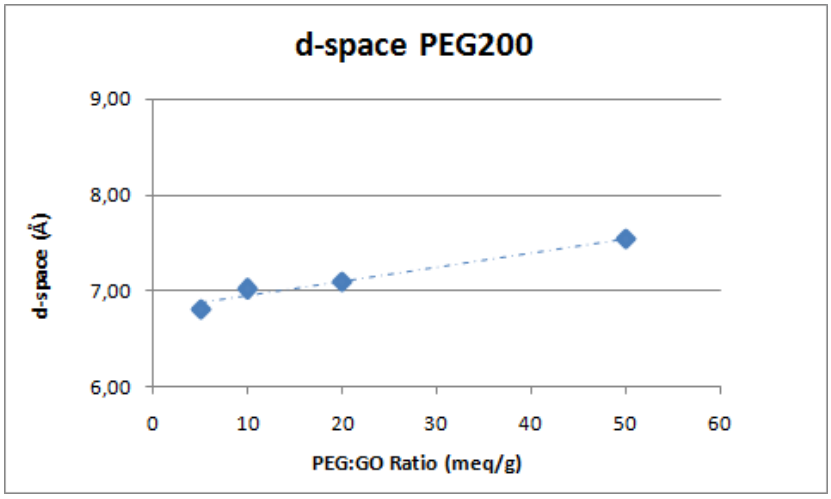

FIGURE 3.6 TREND OF D-SPACE RELATED TO PEG200:GO RATIO

As it is possible to see looking at the Figure 3.7, after 24 hours of tumbling, the water results perfectly clean and the films themselves are undamaged, with the exception of the unmodified GO film that dissolved in water within few minutes. This confirms the increase of GO stability in water following the cross-linking reaction.

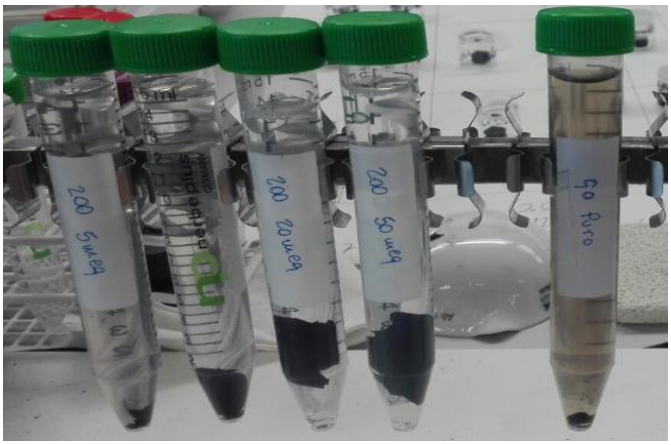

FIGURE 3.7 STATUS OF THE PURE GO AND THE CROSS-LINKED GO FILMS AFTER THE STABILITY TES

In addition, the stability was tested also through the UV-vis Analysis.

PEG 200:GO Ratio (meq/g)	Abs	GO Conc. (g/L)
Pure GO	1.4617	0.1790
5	0.5138	0.0190
10	0.4178	0.0068
20	0.3745	0.0012
50	0.3698	0.0006

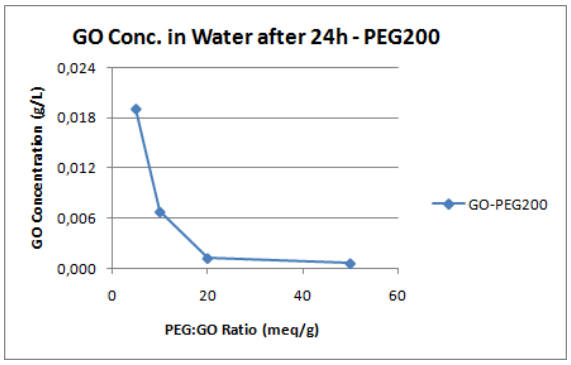

FIGURE 3.8 GO CONCENTRATIONS DISSOLVED IN WATER FOR EACH FILM AFTER STABILITY TEST

As it's possible to see looking at the data above reported in Figure 3.8, each film shows a decrease in the amount of GO dissolved in water (blue line) compared to pure GO. Increasing the amount of PEG 200 used for the cross-linking reaction, the amount of GO dissolved in water continues decreasing, sign of a continuous increase Of GO stability after cross-linking.

In order to study the structural changes, the pieces of free-standing films submerged in water were analyzed again by XRD. This analysis was performed on the samples in *wet condition* and *dry condition* (*paragraph 2.4*). Below, in Figure 3.9, is reported the change in d-space of the films in these conditions compared to the ones before the stability test.

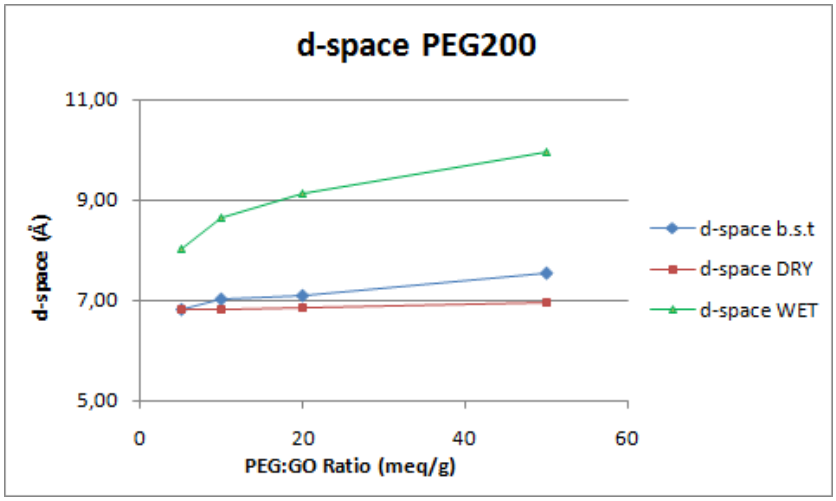

FIGURE 3.9 COMPARISON BETWEEN THE GO D-SPACE FOR EACH FILM ANALYZED IN DRY AND WET CONDITIONS AND THE GO D-SPACE BEFORE STABILITY TESTS (B.S.T)

The thicknesses of the swollen films just after the stability test increases with increasing the amount of PEG (green line), index of an increase of water absorbed between the GO sheets; however, upon subsequent drying (80 °C for one hour), as it is possible to notice looking at the red line, it decreases below those of the films before the stability test, but always remaining higher than the one of unmodified GO. Moreover, this decrease seems to be higher for higher amounts of cross-linker. These results are similar to those of Lecaros *et al.* [35], who observed that the d-spacing of GO increased increasing the amounts of poly(vinyl alcohol) as cross-linker with respect to the pure GO. PEG molecules are linear, and each molecule has only two sites available for cross-linking action. It is reliable that intercalation of increasing amounts of PEG, with a significant fraction of it oriented roughly perpendicularly to the GO layers, progressively increases the space between GO platelets. When submerged in water, the linear PEG molecules can unfold, enabling the films to swell by water uptake. This facilitates the outward diffusion of unreacted cross-linker molecules from the films, which manifests as a reduction of the inter-layer spacing upon drying.

3.2.1.2 PEG 600

The diffractograms reported in Figure 3.10 show, as happened for PEG 200, an increase of d-space compared to the unmodified GO, confirming an interaction between the cross-linker used and the GO sheets. The trend of d-space as a function of cross-linker amount (reported in Figure 3.11) is linear as in the case of PEG 200, nevertheless the slope of the resulting trend is higher than in the previous case, reaching a maximum value of 12,034 Å using 50 meq/g of cross-linker (the analogous value reached using the same amount of PEG 200 was 7,543 Å).

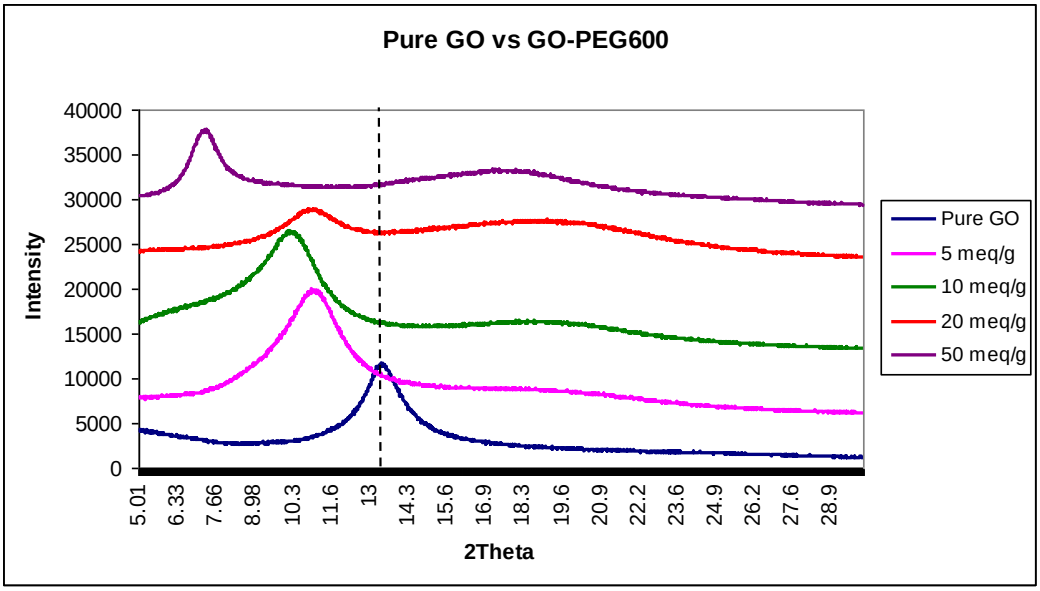

FIGURE 3.10 DIFFRACTOGRAM OF THE FREE-STANDING GO FILMS CROSS-LINKED WITH PEG 600 g/mol

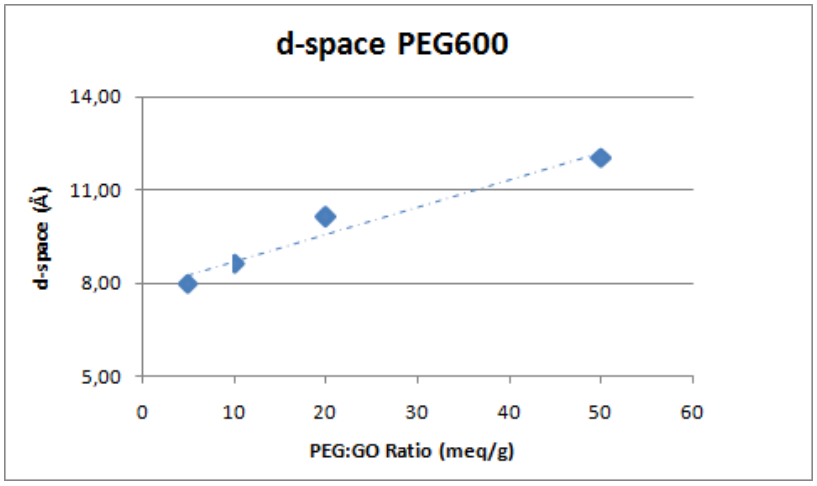

FIGURE 3.11 TREND OF D-SPACE RELATED TO PEG600:GO RATIO

The UV-vis analysis performed on the water containing the fragments of free-standing films after the stability test confirms an increase of GO stability compared to the unmodified one. As a matter of fact, as it is possible to see looking at the data and at in the plot in Figure 3.12, the concentration of GO dissolved in water results to be really low and closed to zero for all PEG 600:GO ratios.

PEG 600:GO Ratio (meq/g)	Abs	GO Conc. (g/L)
Pure GO	1.4617	0.1790
5	0.3818	0.0021
10	0.3808	0.0020
20	0.3759	0.0014
50	0.3745	0.0012

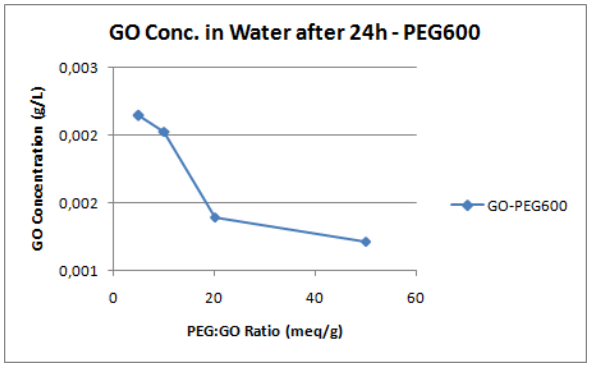

FIGURE 3.12 GO CONCENTRATIONS DISSOLVED IN WATER FOR EACH FILM AFTER STABILITY TEST

The second XRD analysis, performed on the free-standing films after stability test in both wet and dry conditions, led to the results reported in Figure 3.13.

As it is possible to see looking at the green line, there is an increase in d-space after tumbling in water compared to the one of the films before the test (blue line) rteflecting an absorption of water between the GO sheets during the process. The analysis performed on the same films after drying shows a decrease in d-space that becomes lower than that observed before the test. Finally, like in the case already discussed for PEG 200, this decrease is higher increasing the amount of PEG 600 used for the reaction.

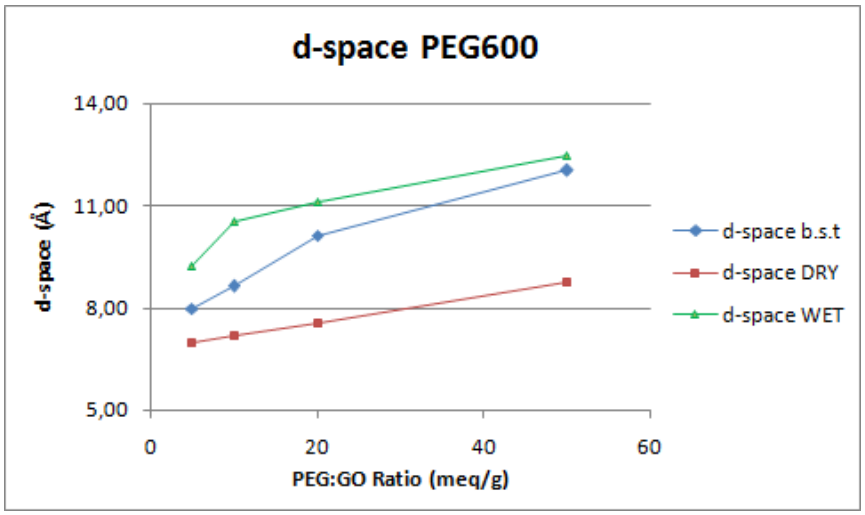

FIGURE 3.13 COMPARISON BETWEEN THE GO D-SPACE FOR EACH FILM ANALYZED IN DRY AND WET CONDITIONS AND THE GO D-SPACE BEFORE STABILITY TESTS (B.S.T)

3.2.1.3 PEG 2000

Looking at the diffractograms reported in Figure 3.14, obtained from the free-standing GO film cross-linked with PEG 2000, it is possible to see an increase in d-space compared to the unmodified GO, confirming that the cross-linking reaction was successful also in this case.

The comparison of the results observed for the three molecular weight PEGs, confirm that the increase in d-space is not only linked to the amount of cross-linker used for the reaction but also to its molecular weight.

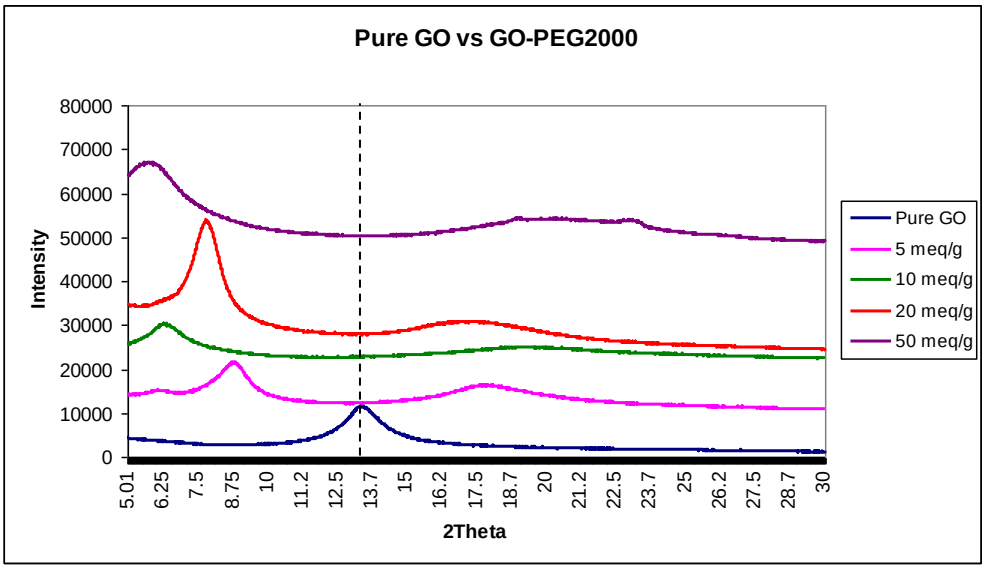

FIGURE 3.14 DIFFRACTOGRAM OF THE FREE-STANDING GO FILMS CROSS-LINKED WITH PEG 2000 g/mol

Figure 3.15 shows that, in the presence of PEG 2000, the trend of d-space as a function of cross-linker amount is not linear anymore, probably indicating that the effect of PEG 2000 presence on d-space reaches a maximum extent that cannot be overcome.

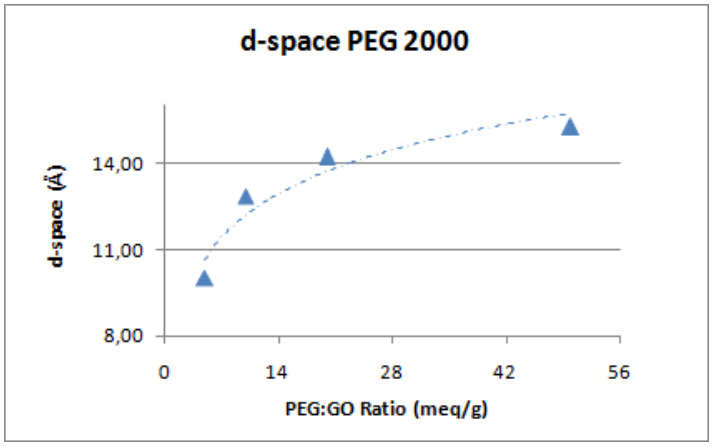

FIGURE 3.15 TREND OF D-SPACE RELATED TO PEG2000:GO RATIO

The UV-vis analysis performed on the free-standing films, objects of the stability test, provided results similar to the other two cross-linkers. As visible from the data in the table and in the plot below (Figure 3.16), the increase of stability is higher than the ones obtained on the free-standing films cross-linked with PEG 200 and 600. Nevertheless, unlike the previous cases, where the amount of GO released in water always decreased with an increase of the amount of the cross-linkers, with PEG 2000 the amount of GO dissolved in water decreases only using low amounts of cross-linker (5 and 10 meq_{PEG}/g_{GO}) while it increases again (indicating a lower stability of GO in water) increasing PEG 2000 amounts. This phenomenon could be related to the effect of PEG 2000 on d-space: probably, GO cannot accommodate a too large amount of high molecular weight PEG. This implies a limited effect on d-space and that the non-reacted excess can be released in water during the stability tests.

PEG 2000:GO Ratio (meq/g)	Abs	GO Conc. (g/L)
Pure GO	1.420	0.1790
5	0.3720	0.0009
10	0.3689	0.0005
20	0.3783	0.0017
50	0.3790	0.0018

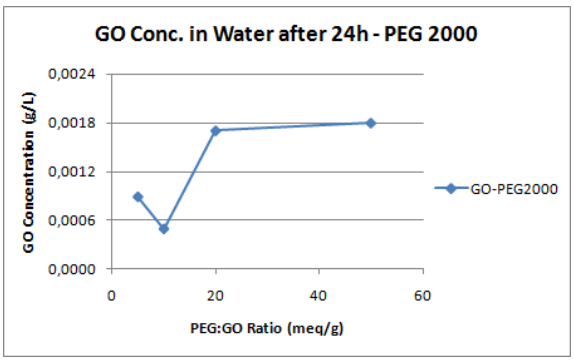

FIGURE 3.16 GO CONCENTRATIONS DISSOLVED IN WATER FOR EACH FILM AFTER STABILITY TEST

As previously, an XRD analysis was performed on the films after the stability test. The results obtained show an increase of d-space of the films analyzed in wet condition that is lower compared to the film cross-linked with PEG at lower molecular weights. This was possible caused by the high molecular weight of this cross-linker that, occupying a lot of space between the GO sheets, prevents an excessive absorption of water. For this reason, analyzing them in dry condition, it was supposed that the d-space value would be back to be really similar to the one it was before the stability test. However, as it is possible to see looking at the red line reported in the plot below, the d-space values for all the films analyzed are really lower compared to the

ones of the film before the stability test. It was assumed that the reason for this phenomenon must be granted again to a non-complete reactivity of PEG with the GO, due to the high molecular weight of the cross-linker. This lack of reactivity could cause a lost of polymer in water during the test but it was not possible to confirm it.

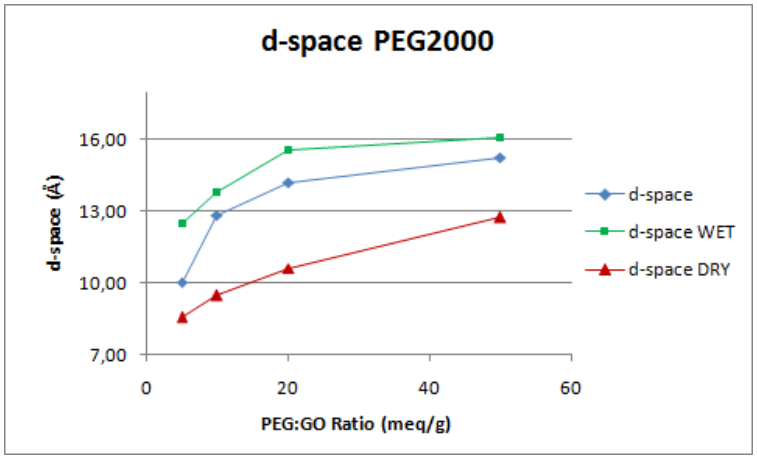

FIGURE 3.17 COMPARISON BETWEEN THE GO D-SPACE FOR EACH FILM ANALYZED IN DRY AND WET CONDITIONS AND THE GO D-SPACE BEFORE STABILITY TESTS (B.S.T)

3.2.1.4 FINAL COMPARISON

It is possible to sum up the results obtained with the three PEGs as follow:

- As it is possible to see in Figure 3.18, the increase of molecular weight causes an increase of the d-space of GO materials. The increase of d-space, increasing with the amount of cross-linker, is linear for PEG 200 and PEG 600 whereas the trend shows a sort of saturation in the case of PEG 2000, as if that molecule cannot be completely hosted by GO.

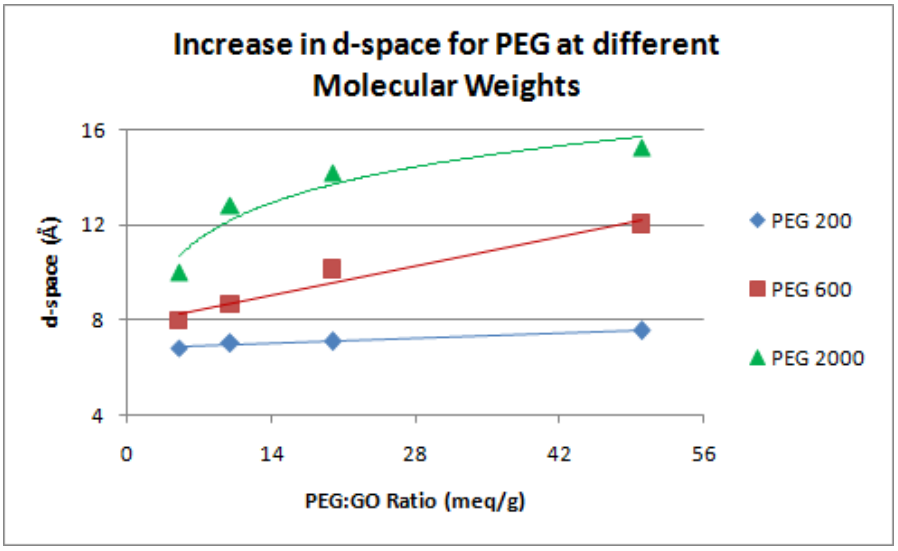

FIGURE 3.18 INCREASE IN D-SPACE FOR PEG AT DIFFERENT MOLECULAR WEIGHTS

- All the three PEG used provide an increase of GO stability in water compared to the unmodified one. Nevertheless, As it is visible in Figure 3.19, for low PEG:GO ratios (5 meq/g and 10 meq/g) an increase of the PEG molecular weight always causes a stabilization of the hybrid materials, whereas for high PEG:GO ratios (20 meq/g and 50 meq/g) the increase of PEG molecular weight causes a destabilization of the hybris materials. This is possibly due to the fact that, as said previously, PEG is a linear molecule with only two sites available for cross-linking reaction. When the amount of high molecular weight PEG becomes too high to be hosted in the GO structure, some PEG remains unreacted and a lack of stability is observed.

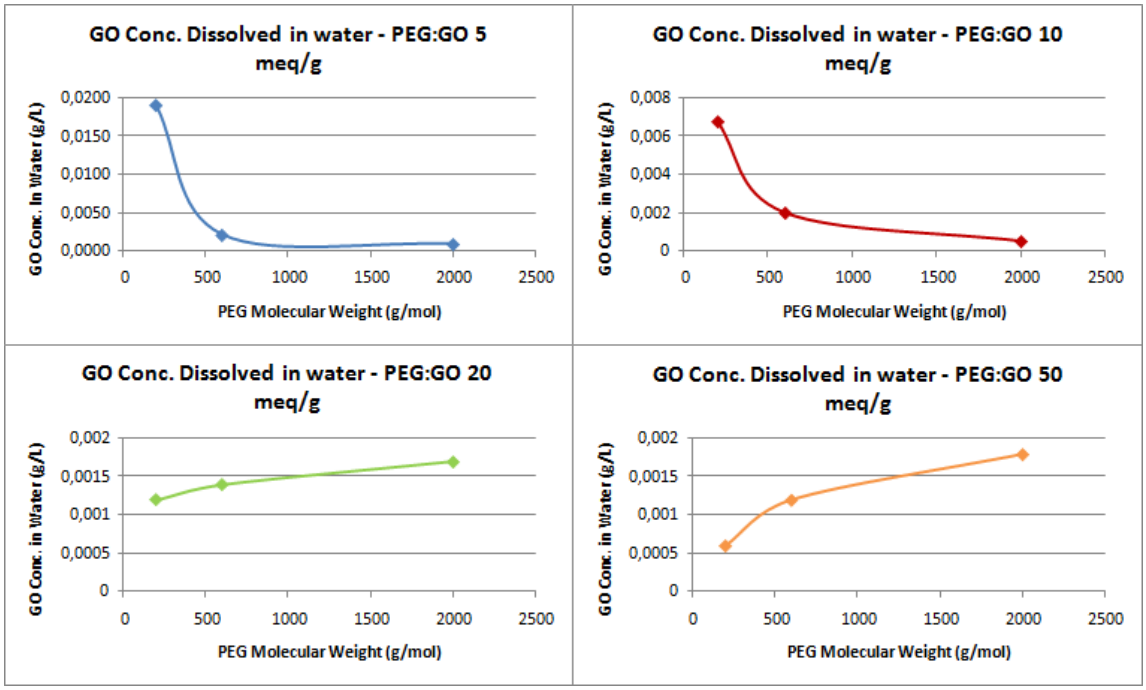

FIGURE 3.19 COMPARISON BETWEEN THE STABILITY TRENDS OF GO CROSS-LINKED WITH PEGs WITH DIFFERENTS MOLECULAR WEIGHT AT THE DIFFERENT PEG:GO RATIOS

3.2.2 SYNTHETIC HYPERBRANCHED POLYOL (HBPO)

HBPO is a synthetic hyperbranched polyol, more precisely it is a compound composed by a Polyethilene Glycol core funtionalized with hydrophilic groups (-OH and –COOH groups). The molecular weight of this polymer is 1750 g/mol and its structure is shown in Figure 3.20.

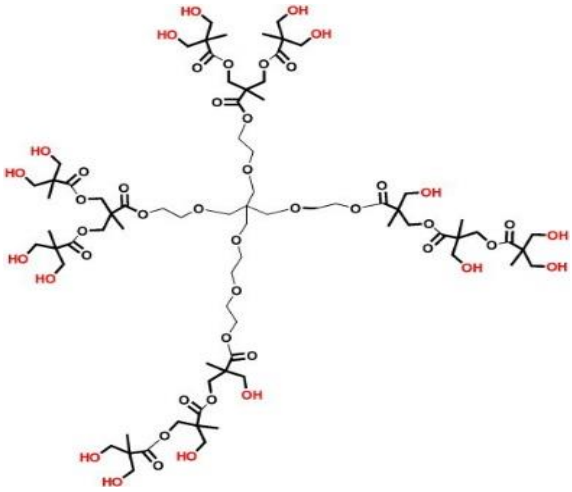

FIGURE 3.20 MOLECULAR STRUCTURE OF HBPO

The XRD analysis performed on the free-standing films cross-linked with this compound confirmed a successful interaction with the GO. As it is possible to see looking at the Figure 3.21 and 3.22, similarly to what happened for PEG 200, the branched polymer causes a limited increase of d-space visible only for the higher HBPO:GO ratio. The reason of this difference is probably due to the branched structure of HBPO, more compact, in terms of steric hindrance, compared to the linear structure of PEG. As a matter of fact, the ramifications added to the PEG core could limit the entanglement degree of the polymer: the cross-linker could position between the GO sheets allowing a limited increase of the space between GO sheets.

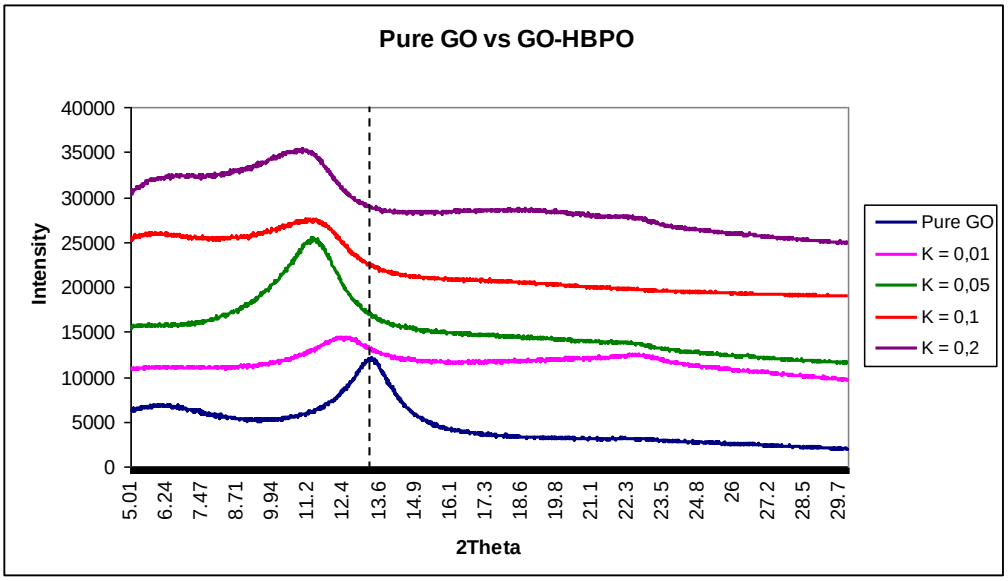

FIGURE 3.21 DIFFRACTOGRAM OF THE FREE-STANDING GO FILMS CROSS-LINKED WITH HBPO

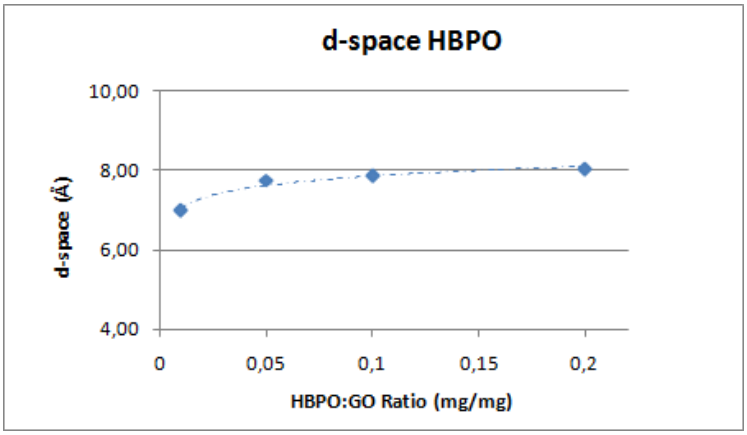

FIGURE 3.22 TREND OF D-SPACE RELATED TO HBPO:GO RATIO

The UV-vis analysis performed on the water containing the free-standing film subjected to the stability test shows that the amount of GO dissolved in water after 24 hours of tumbling is almost the same of PEG 2000 with the difference that for HBPO it is perfectly steady for all the amounts used for stabilize GO, without showing a decrease in stability using high amounts. This can be attributed to the fact that HBPO has multiple -OH groups per molecule, which enable the anchoring of multiple GO platelets together, greatly reducing the solubility of the film in water.

HBPO:GO Ratio (mg/mg)	Abs	GO Conc. (g/L)
Pure GO	1.420	0.179
0.01	0.091	0.005
0.05	0.107	0.007
0.1	0.105	0.006
0.2	0.106	0.007

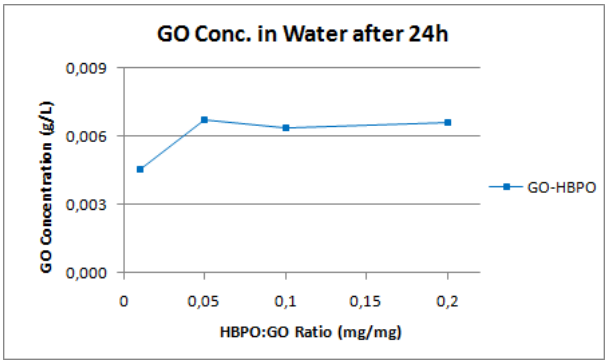

FIGURE 3.23 GO CONCENTRATIONS DISSOLVED IN WATER FOR EACH FILM AFTER STABILITY TEST

Figure 3.24 contains the results obtained performing the XRD analysis on the free-standing films after stability test in both wet and dry condition.

It is possible to see a slight decrease of d-space in wet condition (red line), that indicates a gradual decrease in the amount of water absorbed between the GO sheets increasing the amount of HBPO. As described above, this may be owing to the fact that HBPO has a branched structure, with multiple functional groups per molecule. They can interdigitate with the GO layers, and each molecule can contribute not only to cross-link parallel GO platelets but can also cause cross-linking in plane and between adjacent layers, thus anchoring multiple platelets together. Thus, they form an increasingly enmeshed network at higher loadings, which restricts the swelling of the film.

Also, upon drying, the swelling appears to be almost reversible as the red line in Figure 3.24 results very similar to the blue line relative to the non-treated materials.

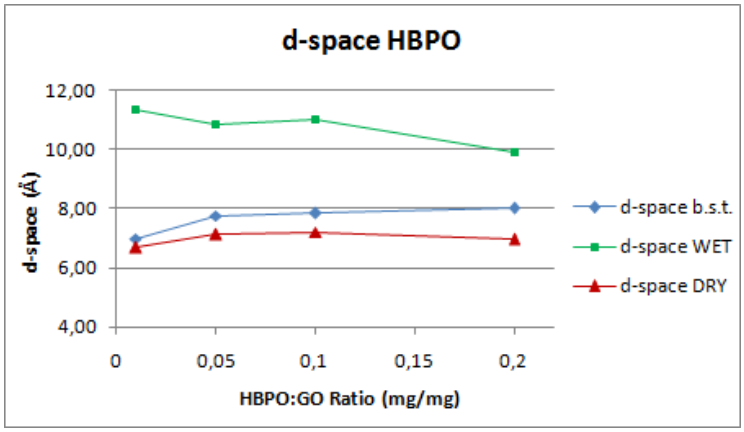

FIGURE 3.24 COMPARISON BETWEEN THE GO D-SPACE FOR EACH FILM ANALYZED IN DRY AND WET CONDITION

3.2.3 HUMIC ACID-LIKE SUBSTANCES (HAL)

Humic substances are organic compounds that are important components of humus, the major organic fraction of soil, peat, and coal. A typical humic substance is a mixture of many molecules, some of which are based on a motif of aromatic nuclei with phenolic and carboxylic substituents, linked together. The functional groups that contribute mostly to surface charge and reactivity of humic substances are phenolic and carboxylic groups.

The HAL used as cross-linker compound in this project was obtained throught an acid/base separation of organic matter deriving from urban waste after composting process. A hypothetical structure of this HAL, drawn basing on several characterization analyses, is reported in Figure 3.25.

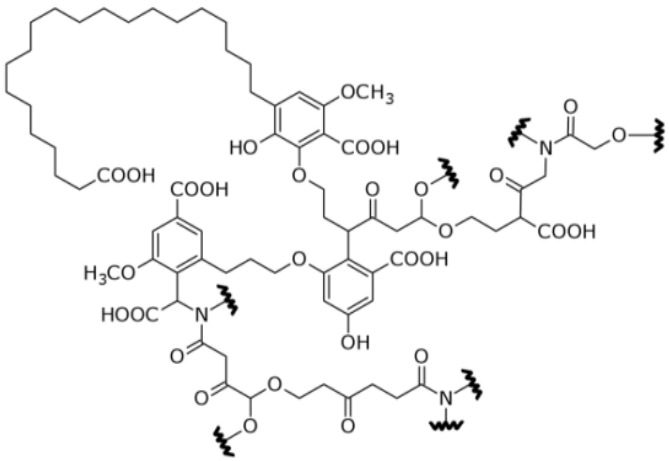

FIGURE 3.25 HYPOTHETICAL MOLECULAR STRUCTURE OF HAL

The XRD analysis performed on the films cross-linked with HAL at different HAL:GO ratios shows a random change of the 2Theta value, corresponding to a random variations of d-space, as it is possible to see in Figures 3.26 and 3.27. Unlike the previous cases, therefore, the changes observed do not correspond to specific trends.

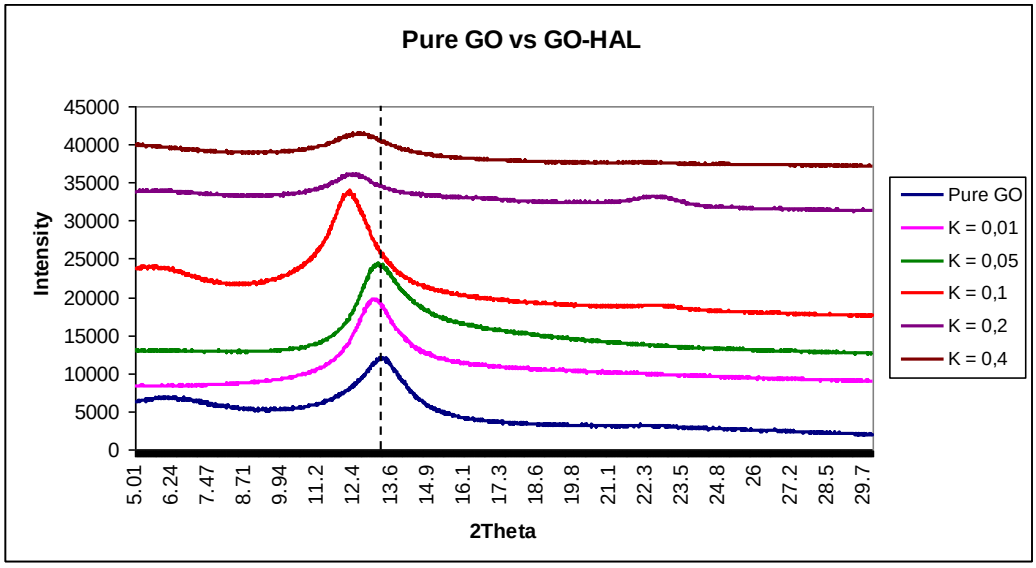

FIGURE 3.26 DIFFRACTOGRAM OF THE FREE-STANDING GO FILMS CROSS-LINKED WITH HAL

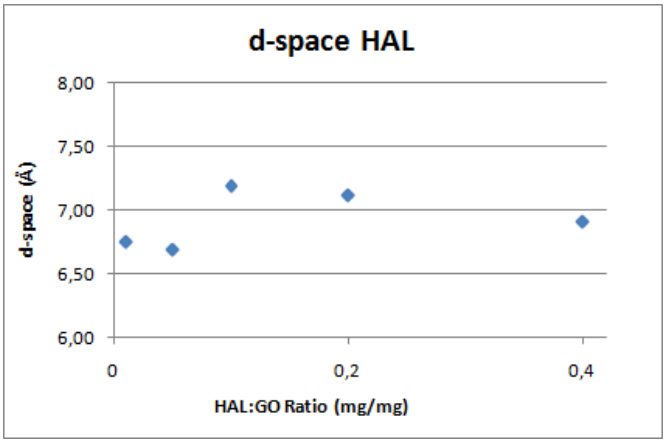

FIGURE 3.27 TREND OF D-SPACE RELATED TO HAL:GO RATIO

The results obtained through the UV-vis analysis performed on the water used for the stability test are reported in Figure 3.28. Also in this case the cross-linker increases the stability of GO but only when HAL is used in high ratios (higher than HAL:GO > 0.01). In any case, the stability observed is lower than that observed in the case of PEGs and HBPO.

HAL:GO Ratio (mg/mg)	Abs	GO Conc. (g/L)
Pure GO	1.423	0.179
0.01	1.811	0.230
0.05	0.556	0.065
0.1	0.471	0.054
0.2	0.441	0.050
0.4	0.305	0.033

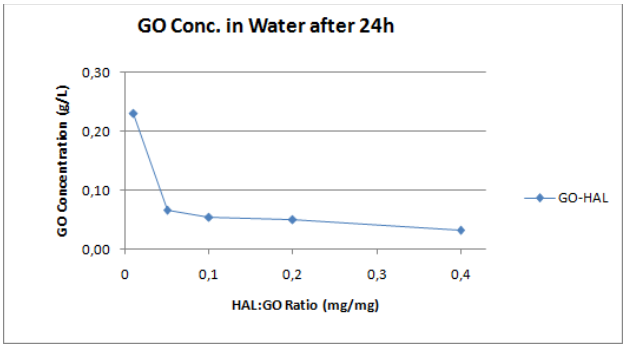

FIGURE 3.28 GO CONCENTRATIONS DISSOLVED IN WATER FOR EACH FILM AFTER STABILITY TEST

The results obtained analyzing the swollen free-standing films after the stability test show a great increase in d-space in wet condition, index of an extended absorption of water (red line). Otherwise, after drying process, the values come back to the ones the films had before being submerged in water, indicating a perfectly reversible process.

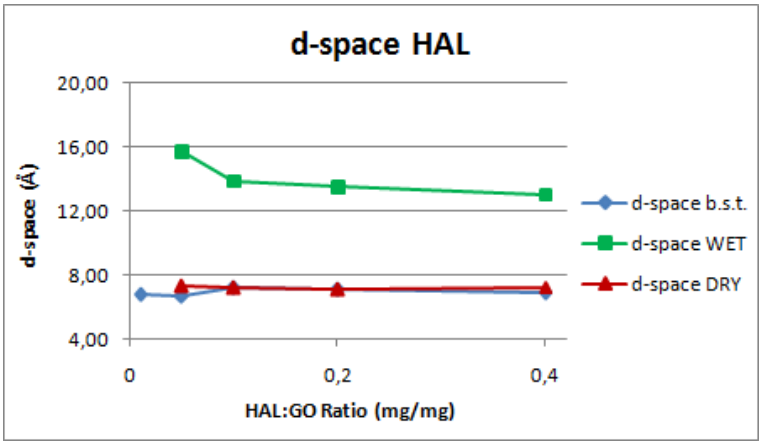

FIGURE 3.29 COMPARISON BETWEEN THE GO D-SPACE FOR EACH FILM ANALYZED IN DRY AND WET CONDITION

As a conclusion of this section, it was chosen to carry out the permeation tests with the samples which showed the highest stability in water, *i.e.*

- HBPO:GO 0.2 mg/mg
- HAL:GO 0.4 mg/mg
- PEG 2000:GO 5 meq/g (corresponding to 5 mg/mg)

PEG 2000 was chosen not only for the stability in water it gave to GO layer, but also cause its molecular weight is really similar to those of the other two cross-linkers. This led us to have a good comparison between linear and branched molecules.

An unmodified GO film was used as comparison.

3.3 VAPOUR PERMEATION EXPERIMENTS

For the separation experiments, four large-area supported GO films were produced as described in *paragraph 2.5*.

Figure 3.30 reports the SEM images of GO and HBPO-GO films supported on polyethersulphone membrane.

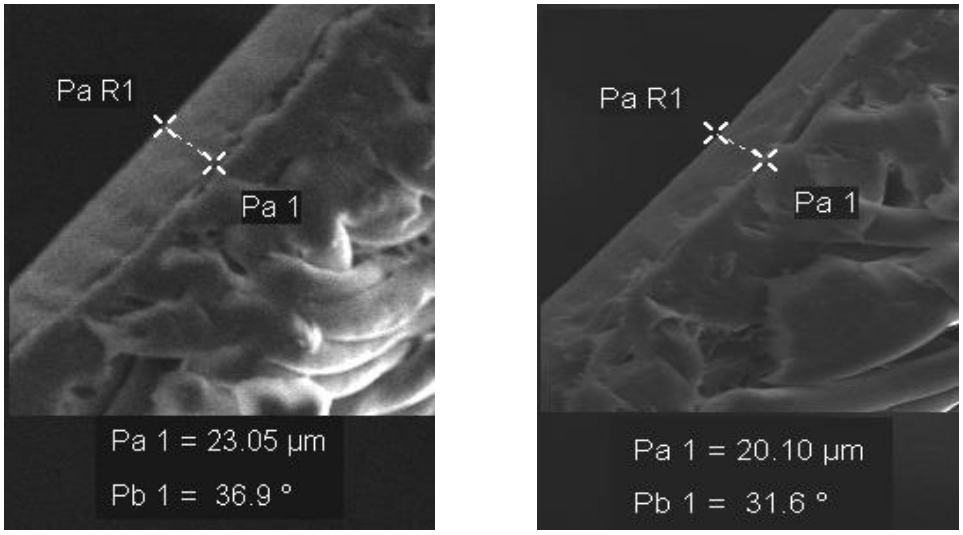

FIGURE 3.30 SEM IMAGES – THICKNESS OF THE GO LAYER ON THE POLYETHERSULPHONE MEMBRANE

In both cases, the thickness of the GO layers deposited on the support are similar (23,05 µm for the unmodified GO and 20,10 µm for the cross-linked one), index of a good reproducibility of the Meyer rod coating method. This will allow us to exclude, during the permeation experiments, experimental errors due to a different thockness of the active layer.

Figure 3.31 reports the SEM images obtained from the same samples at higher magnification. It seems that the introduction of the cross-linker between the GO sheets led to a more ordered and organized disposition of the platelets compared with the structure of the active layer corresponding to the membrane with the unmodified GO, that shows a clearly more disordered structure. This could be due to the fact that the new bonds, formed as a result of the cross-linking reaction between the GO layers and the stabilizing species organizes the different layers in a more ordered arrangement.

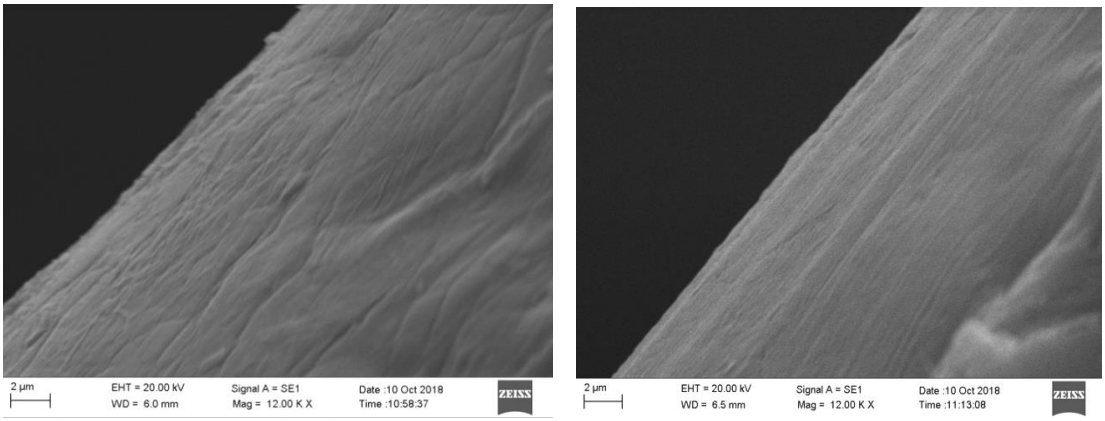

FIGURE 3.31 SEM IMAGES – FOCUS ON THE STRUCTURE OF THE GO LAYER ON THE POLYETHERSULPHONE MEMBRANE

3.3.1 PERMEATION OF WATER AND ETHANOL

The control set-up using a non-permeable aluminum foil showed no weight loss for either water or ethanol, confirming that the set-up did not suffer any leakage.
The normalized weight loss (*i.e.*, weight loss per unit area of membrane) of water at various time intervals, and the flux, *J*, of water and ethanol determined from the weight loss for the four types of GO membranes (unmodified and cross-linked by HAL, HBPO and PEG2000) at various temperatures are shown in Figure 3.32.

The normalized weight loss of water for each type of membrane and at each temperature can be fitted to a straight line (with a minimum R2 value of 0.997), establishing that the membranes, even the pure GO one, did not show significant structural changes during our tests. Moreover, the figure shows good reproducibility of the data even when tests were conducted over three different membrane samples.

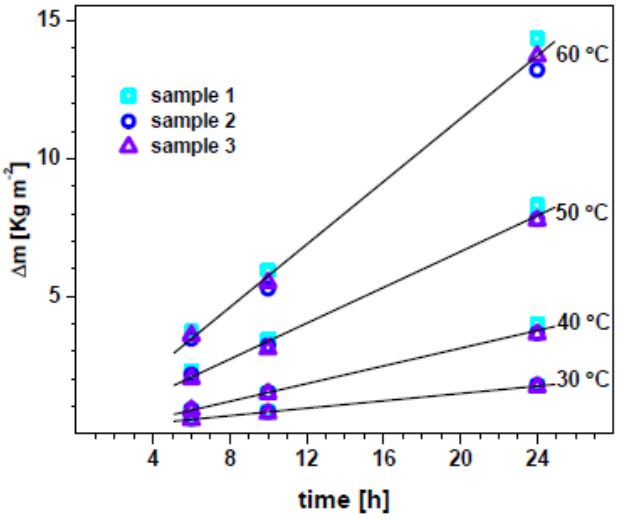

FIGURE 3.32 NORMALIZED WEIGHT LOSS OF WATER AT VARIOUS TIME INTERVALS OVER THREE DIFFERENT MEMBRANE SAMPLES

The molar flux of both water and ethanol, shown in Figure 3.33, for the unmodified and HAL- and HBPO-cross-linked membrane are throughout higher than those for PEG2000-crosslinked GO. This may imply that, in spite of higher d-space achieved by the PEG 2000, the macromolecules hinder the passage of water and ethanol through the membrane. Nevertheless, it may be possible to achieve higher permeance by using a lower amount of PEG, or PEG with lower molecular weight. Studies are underway to determine if higher flux and permeance can be achieved by using polymer membranes of higher porosity, such as microfiltration membranes.

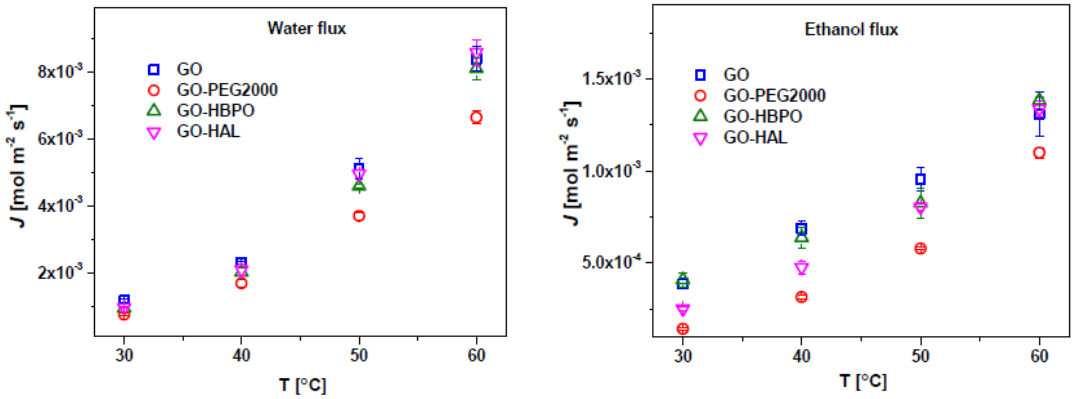

FIGURE 3.33 MOLAR FLUX FOR WATER AND ETHANOL AT DIFFERENT TEMPERATURE FOR THE DIFFERENT MEMBRANES

The apparent Activation Energy relative to vapor permeation process, *Ea*, is determined from the Arrhenius plot that reports ln(*J/p*) versus the reciprocal of *RT* [36], where:

- ***J*** is the Molar Flux (mol/m²*s);
- ***p*** is the Partial Pressure (Pa);
- ***R*** is the Gas Constant (8,31 J/mol*K);
- ***T*** is the Absolute Temperature (K)

The results obtained for water and ethanol for all the membranes under study are shown in Figure 3.34

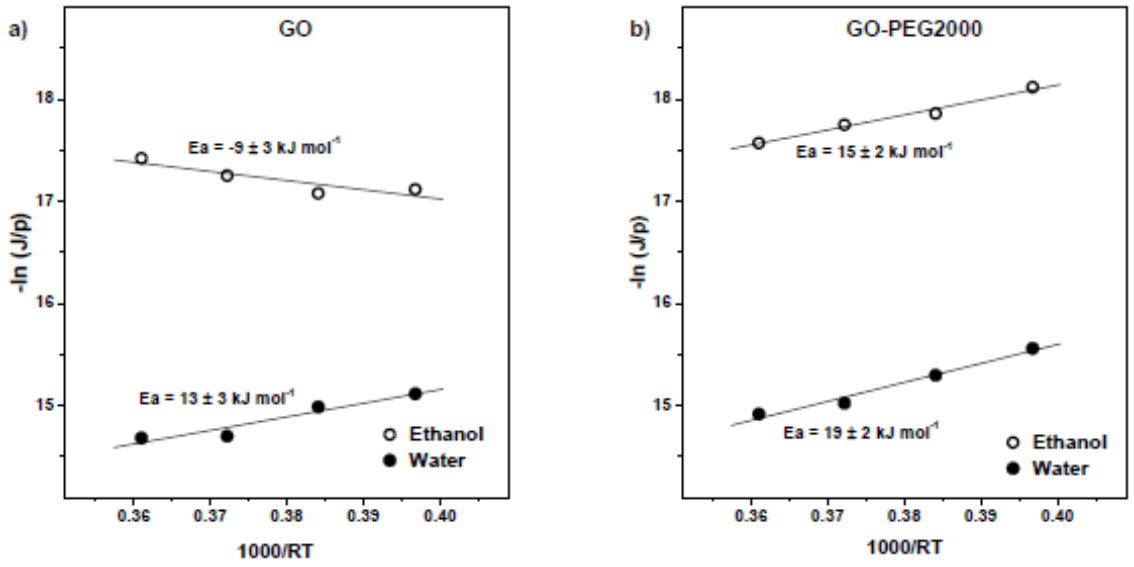

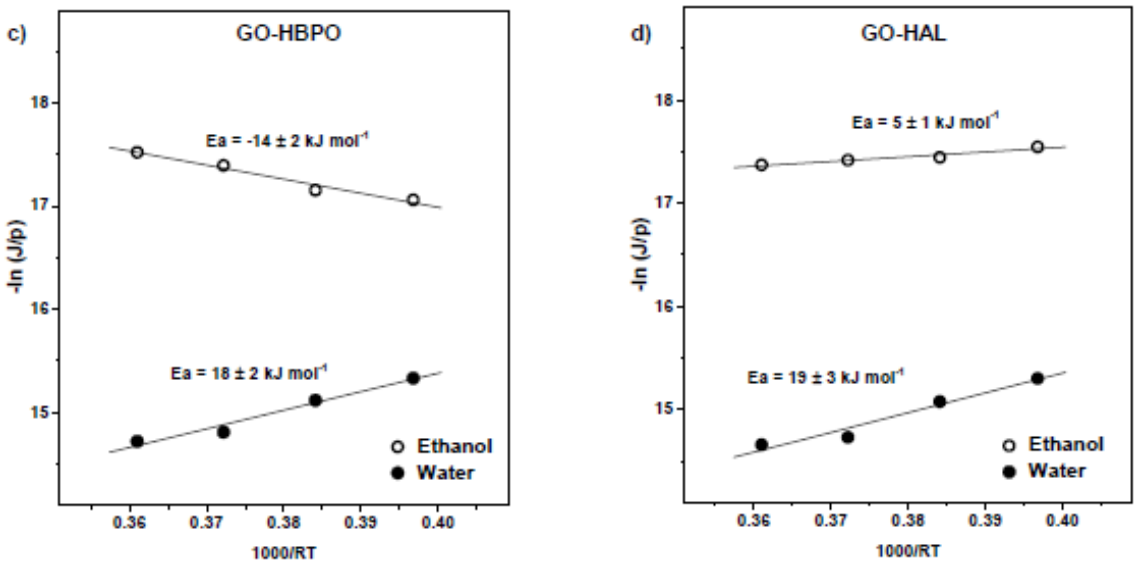

FIGURE 3.34 APPARENT ACTIVATION ENERGY (Ea) RELATIVE TO VAPOR PERMEATION PROCESS FOR THE DIFFERENT MEMBRANES

The Ea values calculated in this study are similar to those determined by Suhas *et al.* for pervaporation of isopropanol/water mixture through a composite membrane of graphene and sodium alginate [37]. The almost similar values for both GO and graphene seems to corroborate the hypothesis that water molecules slide without hindrance over the hydrophobic regions of the sheets [38].

While the *Ea* values for ethanol are negative for unmodified GO and GO-HBPO, they are positive for GO-HAL and GO-PEG2000. This may be owing to the fact that the oxygen-containing functional groups in GO, as well as the surplus hydroxyl groups in HBPO, bind with the ethanol, whereas in GO-HAL and GO-PEG, such sites are not available for binding as they are masked by the cross-linker moieties. For GO-PEG2000, the values of *Ea* for water and ethanol are very similar. This may be the reason behind the poor water ethanol selectivity of GO-PEG2000 membrane.

At this point it is possible to calculate the permeance for both water and ethanol through the membranes, normalizing the flux for their vapor pressure at the different temperatures.

Known the permeance, it is also possible to calculate a theoretical selectivity (α). More precisely, it can be calculated following to different methods:

- A **Predictive Method** that lets us predict the selectivity at different temperatures, also higher than 60 °C, via the solution-diffusion mechanism by the use of solubility and diffusivity models [39];
- An **Experimental Method** whereby selectivity is calculated using the permeance of water and ethanol previously calculated.

$$\alpha = {Permeance_{Water}}/{Permeance_{Ethanol}}$$

The results obtained using these two methods are reported in Figure 3.35:

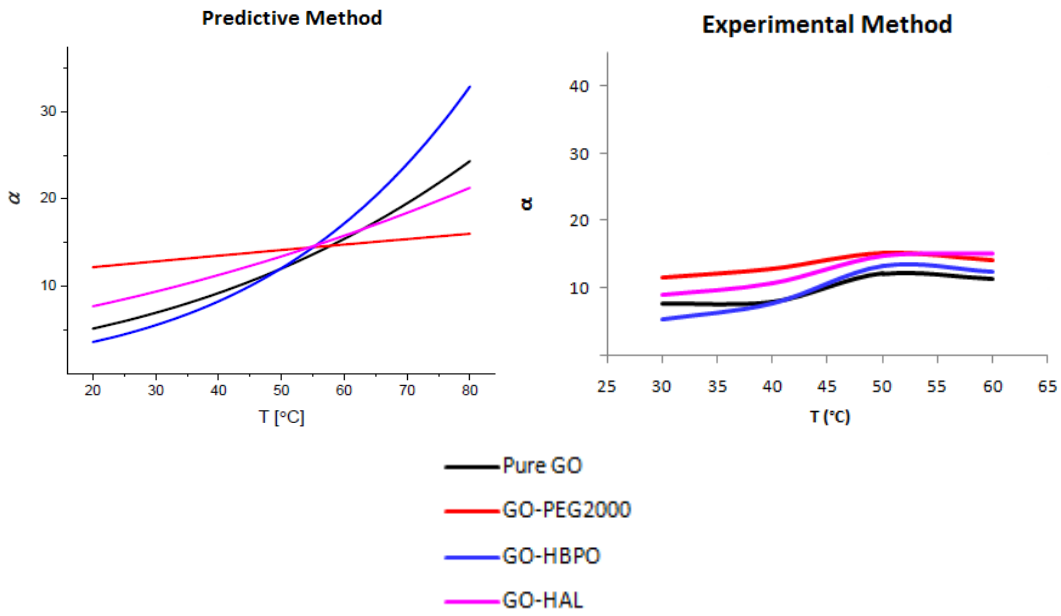

FIGURE 3.35 WATER/ETHANOL SELECTIVITY, RELATED TO THE TEMPERATURE, FOR EACH MEMBRANE, OBTAINED THROUGH THE PREDICTIVE AND THE EXPERIMENTAL METHOD

Looking at the plot obtained with the predictive method, the selectivity of all membranes for all temperatures increase exponentially with temperature. The only

exception is the selectivity of GO-PEG 2000 that shows a really low increase in α with an almost linear trend, as expected considering the Ea for water and ethanol obtained with this membrane.

The trend of selectivity obtained with the experimental method is not so different from the ones obtained with the predictive method: GO-PEG 2000 membrane selectivity change in a very limited extent with respect to the others, whereas GO, GO-HBPO and GO-HAL selectivity increases almost exponentially, at least for the low temperature range. The difference between predictive and experimental methods in the high temperature range seems to derive from an experimental limitation. In fact, all the membranes fixed on ethanol bottles warp at 60 °C, probably giving leakage issues. Basing on these results, all the experiments with water/ethanol mixture were carried out at a temperature not higher than 50 °C.

3.3.2 DEHYDRATION OF WATER/ETHANOL MIXTURE

The composition of the retentate in the bottles after 24 h of vapor permeation at 50°C for pure GO and the three cross-linked supported membranes are shown in Figure 3.36. The results show that, in all cases, the membranes are able to dehydrate the ethanol water beyond the azeotropic point at 1 atm, corresponding to a composition of 95.6 weight % ethanol (Figure 3.36a). Figure 3.36b compares the permeate flux measured for pure water and pure ethanol, with that obtained for the ethanol/water mixture. As expected, the permeate flux observed in the case of the mixture is similar to that observed for absolute ethanol.

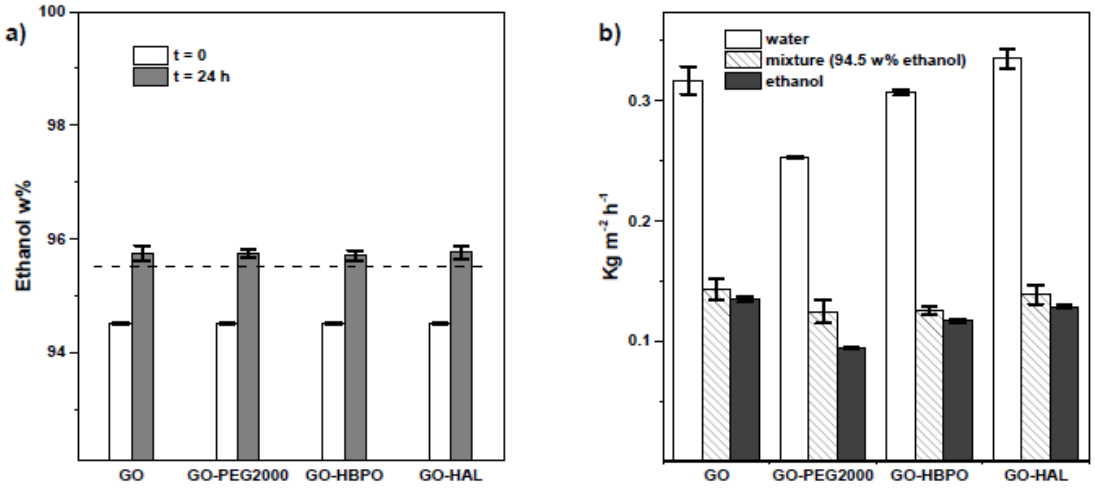

FIGURE 3.36 (a)COMPOSITION OF THE RETENTATE IN THE BOTTLES AFTER 24h AT 50 °C (b) PERMEATE FLUX FOR PURE WATER AND ETHANOL AND FOR THE MIXTURE

From the weight loss and the initial and final compositions of the mixtures in the bottle, the average composition of the permeate was calculated and used to calculate the real water/ethanol selectivity. To carry out these calculations, some simplifications were considered:

1. The possibility that water and ethanol could be absorbed by the membranes was not taken in account, therefore the liquid composition difference in the mixture before and after the test corresponds to the composition of the vapor passed through the membranes

2. The water/ethanol mixture was considered ideal, with no interactions between the molecules, therefore the total pressure in the bottle was calculated as the sum up of the partial pressure of the single components at 50 °C normalized on the vapor composition calculated as described in the previous point.

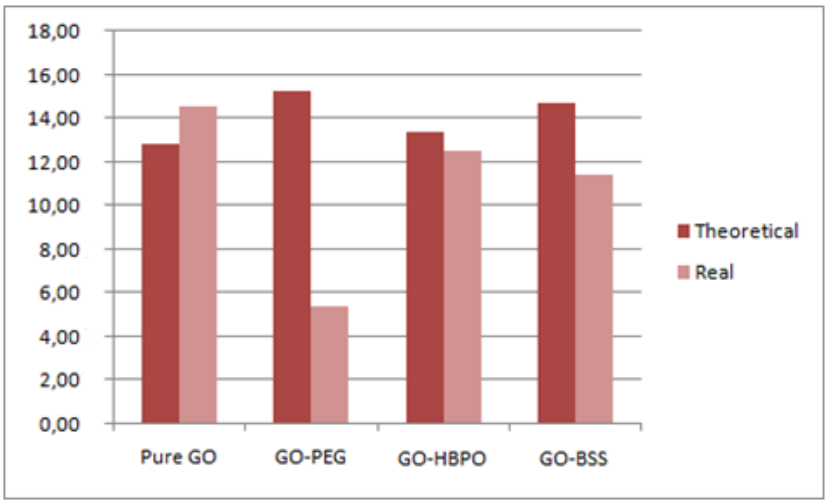

FIGURE 3.37 COMPARISON BETWEEN IDEAL AND REAL WATER/ETHANOL SELECTIVITY

According to the results obtained and reported in Figure 3.37, the real selectivities were always lower than theoretical ones, probably because the starting hypotheses were too limitating. Moreover, it is possible to suppose that the differences between the real selectivities comparing the different membranes are essentially caused by the different spaces between the GO layers: narrow spaces between the layers allow a more efficient separation differently from layers placed at a greater distance.
The main conclusions deriving from data analysis can be summarized as follow:

- The d-space corresponding to the unmodified GO is lower than the other membranes stabilized with the cross-linkers and, as a matter of fact, the real selectivity results to be the highest compared to the others;

- The ideal selectivity of GO-PEG membrane is the lowest. The d-space between GO layers of the membrane cross-linked with PEG at the chosen composition corresponds to a value around 11,5 Å, the highest compared to the d-space obtained with the other two cross-linkers, corroborating the assumption made above. Due to the interactions between water and ethanol, combined with high d-space, the real selectivity is also really different from the ideal one;

- The d-spaces corresponding to the GO membranes cross-linked with HBPO and HAL are really similar and not so much higher compared with the one of the unmodified GO. As result, the selectivity in these two cases are similar to that obtained for the unmodified GO.

4. CONCLUSIONS

We have reported the stabilization of GO films by the use of cross-linking species. In detail, we studied the effect of branched cross-linkers, a humic-acid like substance derived from urban waste compost and a synthetic hyperbranched polyol, and the linear diol Polyethylene Glycol with different molecular weights (from 200 to 600 to 2000 g/mol). The effect of the amount of cross-linkers added to GO was studied.
The success of the cross-linking process was tested via XRD.
The stability of the films was checked considering the release of GO in water after 24 hours tumbling and the swelling properties observed after immersion of the films in water and after subsequent heating.
As a result of these tests, we concluded that:

- All the GO cross-linked films, with the exception of the the GO-HAL film with HAL:GO ratio 0.01, results actually stabilized by the cross-linkers;

- The HBPO was able to stabilize GO films even in very low amounts (HBPO:GO Ratio = 0.01), which may be attributed to its branched structure and multiple -OH groups per molecule, which facilitates interdigitation of the GO platelets;

- The two species with a branched structure used as cross-linkers led to a continue increase in stability of the free-standing GO films with an increase in Cross-Linker-GO ratio. Different is the behaviour of PEG that led to an increase in stability with an increase in its amount only for lower molecular weight while, using PEG 2000 g/mol, the stability of GO decrease with an increase of PEG:GO ratio.

The most stable hybrid materials were chosen and coated on a commercially available polyethersulphone membrane, using the Meyer Rod coating method, to obtain large area films (this method could be suitable for scaling up the preparation

process for market applications). The resulting membranes were tested in vapor permeation experiments with water, ethanol and their mixture.
Single-vapor permeation experiments showed that:

- Cross-linkers can affect water/ethanol selectivity of GO membranes compared to the ones produced with unmodified GO;

- According to the predictive method, selectivity increases exponentially with temperature for GO membranes produced using branched molecules. All these membranes show a selectivity higher than that of the unmodified GO one at high temperature, whereas the use of PEG 2000 as cross-linker allows to increase the selectivity with respect to the one of pure GO only at low temperature.

The final tests carried out to demonstrate the potential applicability of these films in ethanol dehydration via vapor permeation show that:

- All the tested membranes were able in dehydrating ethanol, in fact in all cases retentate shows an ethanol fraction larger than the azeotropic composition;

- Concerning the selectivity, the predictive method allows to obtain reliable indications, in particular for the branched cross-linker HBPO and HAL, whereas the selectivity of the PEG cross-linked membrane results much lower than the expected results, probably because the large space between GO sheets, observed for that film, allows an easy passage of water and ethanol together through the membrane.

Based on these results, the cross-linking procedure results an easy-to-perform and efficient method to achieve self-standing GO membranes useful for ethanol dehydration.

REFERENCES

[1] V. Boffa *et al.* Carbon-based building blocks for alcohol dehydration membranes with disorder-enhanced water permeability. *Carbon* **118** (2017), pp. 458-466

[2] Jinxia Ma, Dan Ping and Xinfa Dong. Recent Developments of Graphene Oxide-Based Membranes: A Review. *Membranes* **7**, 52 (2017)

[3] N.H. Afghan. Sustainability Concept for Energy, Water and Environment Systems. In: Hanjalić K., Van de Krol R., Lekić A. (eds) *Sustainable Energy Technologies* (2008), pp. 25-49

[4] A. Evans, V. Strezov, T.J. Evans. Assessment of Sustainability Indicators for Renewable Energy Technologies. *Renewable and Sustainable Energy Reviews* **13** (2009), pp. 1082-1088

[5] W. Kujawski. Application of Pervaporation and Vapor Permeation in Enviromental Protection. *Polish Journal of Environmental Studies* **9** (2000), pp. 13-26

[6] Renewables 2015 — Global Status Report, Renewables Academy (2015)

[7] Ngoc Lieu Le, Suzana P. Nunes. Materials and membrane technologies for water and energy sustainability. *Sustainable Materials and Technologies* **7** (2016), pp. 1–28

[8] Saeid Baroutian *et al.*. Methanol recovery during transesterification of palm oil in a TiO2/Al2O3 membrane reactor: Experimental study and neural network modeling. *Separation and Purification Technology* **76** (2010), pp. 58–63

[9] Saeid Baroutian *et al.* A packed bed membrane reactor for production of biodiesel using activated carbon supported catalyst. *Bioresource Technology* **102** (2011), pp. 1095–1102

[10] L. Guerreiro *et al.* Transesterification of soybean oil over sulfonic acid functionalised polymeric membranes. *Catalysis Today* **118** (2006), pp. 166–171

[11] Subhankar Basu *et al.* Membrane-based technologies for biogas separations. *Chemical Society Reviews* **39** (2010), pp. 750-768

[12] S. Rasi, A. Veijanen, J. Rintala. Trace compounds of biogas from different biogas production plants. *Energy* **32 (8)** (2007), pp. 1375-1380

[13] Tai-Shung Chung, Lan Ying Jiang, Yi Li, Santi Kulprathipanja. Mixed matrix membranes (MMMs) comprising organic polymers with dispersed inorganic fillers for gas separation. *Progress in Polymer Science* **32** (2007), pp. 483–507

[14] Siti Hajar Mohd Azhar *et al.* Yeasts in sustainable bioethanol production: A review. *Biochemistry and Biophysics Reports* **10** (2017), pp. 52–61

[15] Ping Wei et al. A review of membrane technology for bioethanol production. *Renewable and Sustainable Energy Reviews* **30** (2014), pp. 388-400

[16] N. Rossi, P. Jaouen, P. Legentilhomme And I. Petit. Harvesting Of Cyanobacterium Arthrospira Platensis Using Organic Filtration Membranes. *Food and Bioproducts Processing* **82** (2004), pp. 244-250

[17] Jingwen Che net *al.* Removal of inhibitors from lignocellulosic hydrolyzates by vacuum membrane distillation. *Bioresource Technology* **144** (2013), pp. 680–683

[18] Karthikeyan Krishnamoorthy, Murugan Veerapandian, Kyusik Yun, S.-J. Kim. The chemical and structural analysis of graphene oxide with different degrees of oxidation. *Carbon* **53** (2013), pp. 38–49

[19] Da Chen, Hongbin Feng and Jinghong Li. Graphene Oxide: Preparation, Functionalization, and Electrochemical Applications. *Chem. Rev.* **112 (11)** (2017), pp. 6027-6053

[20] B.C. Brodie. On the Atomic Weight of Graphite. *Philosophical Transactions of the Royal Society of London* **149** (1859), pp. 249-259

[21] William S. Hummers, Jr., and Richard E. Offeman. Preparation of Graphitic Oxide. *J. Am. Chem. Soc.* **80 (6)**, pp. 1339–1339

[22] Nina I. Kovtyukhova *et al.* Layer-by-Layer Assembly of Ultrathin Composite Films from Micron-Sized Graphite Oxide Sheets and Polycations. *Chem. Mater.* **11** (1999), pp. 771-778

[23] Marcano *et al.* Improved Synthesis of Graphene Oxide. *ACS Nano* **4 (8)** (2010), pp. 4806-4814

[24] Li Peng *et al.* An iron-based green approach to 1-h production of single-layer graphene oxide. *Nature Communications* **6 (5716)** (2015), pp. 1-9

[25] Mohammad Rafi, Babak Samiey and Chil-Hung Cheng. Study of Adsorption Mechanism of Congo Red on Graphene Oxide/PAMAM Nanocomposite. *Materials* **11** (2018), pp. 1-24

[26] Wenhua Chen *et al.* The preparation and application of a graphene-based hybrid flame retardant containing a long-chain phosphaphenanthrene. *Scientific Reports* **7 (8759)** (2017), pp. 1-12

[27] Kyoung Hoon Chu *et al.* Evaluation of graphene oxide-coated ultrafiltration membranes for humic acid removal at different pH and conductivity conditions. *Separation and Purification Technology* **181** (2017), pp. 139–147

[28] Mingchao Zhang *et al.* Sheath–Core Graphite/Silk Fiber Made by Dry-Meyer-Rod-Coating for Wearable Strain Sensors. *ACS Appl. Mater. Interfaces* **8** (2016), pp. 20894–20899

[29] Liangbing Hu *et al.* Scalable Coating and Properties of Transparent, Flexible, Silver Nanowire Electrodes. *ACS Nano* **4 (5)** (2010), pp. 2955-2963

[30] Jie Wang et al. Rod-Coating: Towards Large-Area Fabrication of Uniform Reduced Graphene Oxide Films for Flexible Touch Screens. *Advanced Materials* **24 (21)** (2012), pp. 2874-2878

[31] Zhao, J.; Zhu, Y.; Pan, F.; He, G.; Fang, C.; Cao, K.; Xing, R.; Jiang, Z. Fabricating graphene oxide-based ultrathin hybrid membrane for pervaporation dehydration via layer-by-layer self-assembly driven by multiple interactions. *J. Membr. Sci.* **487** (2015), 162–172

[32] Euntae Yang et al. Enhanced desalination performance of forward osmosis membranes based on reduced graphene oxide laminates coated with hydrophilic polydopamine. *Carbon* **117** (2017), pp. 293-300

[33] Cote L.J., Kim F., Huang J. Langmuir-Blodgett Assembly of Graphite-Oxide Single Layers. *J. Am. Chem. Soc.* **131** (2009), pp. 1043-1049

[34] Wufeng Chen, Lifeng Yan. Preparation of Graphene by a Low-Temperature Thermal Reduction at Atmosphere Pressure. *Nanoscale* **2** (2010), pp. 559-563

[35] Lecaros *et al.* Tunable Interlayer Spacing of Composite Graphene Oxide-Framework Membrane for Acetic Acid Dehydration. *Carbon* **123** (2017), pp. 660-667

[36] Xianshe Feng, Robert Y.M., Huang. Estimation of Activation Energy for Permeation in Pervaporation Processes. *Journal of Membrane Science* **118** (1996), pp. 127.131

[37] Suhas *et al.* Graphene-loaded Sodium Alginate Nanocomposite Membranes with Enhanced Isopropanol Dehydration Performace via a Pervaporation Technique. *RSC Advances* **3 (38)** (2013), pp. 17120-17130

[38] Boukhvalov DW, Katsnelson MI, Son YW. Origin of Anomalous Water Permeation through Graphene Oxide Membrane. *Nano Lett.* **13 (8)** (2013), pp. 3930-3935

[39] S.J. Doong , W.S. Ho, R.P. Mastondrea. Prediction of flux and selectivity in pervaporation through a membrane. *Journal of Membrane Science* **107** (1995), pp. 129-146

ACKNOWLEDGMENTS

First of all, I would like to express my sincere gratitude to my supervisor, Prof.ssa Giuliana Magnacca, for her continuous encouragement, patience, and assistance throughout the development of this thesis, and without whom this work would have been much different. In addition, I would also like to thank Prof. Vittorio Boffa and Dr. Anil Suri for their precious help and advice in the project development during my stay in Aalborg.

I would have never made it this far in these years, if it were not for my parent's and my brother's strength and my family's support, which I will never thank enough. I would like to thank my best friends Giulia and Francisco and my friends Federico, Giulia, Martina, Maurizio, Alberto, Silvia, Gloria, Marta and Claudia for their encouraging words and the support they gave me so far.

I would also like to thank Elisa, Elena, Francesco, Francesco and Alessandro who have been the best fellow adventurer I could hope for during my stay in Aalborg.

A final thank you goes to Giorgia, my girlfriend, who has been there for me in the last steps of this path sustaining and encouraging me in every possible way.